CHAPTER IV
RESULTS AND DISCUSSION

BC has been used for various applications including food applications. This work aims to develop the novel films from the blend of BC, sodium alginate and gelatin (BAG) for further application as food packaging materials. In order to improve the physical and functional antimicrobial properties of the film, it was incorporated with glycerol/ sorbitol as plasticizer, tannic acid as cross-linking and antimicrobial agent and mangosteen ethanolic extract as antimicrobial agent. The effects and the optimal content of the supplement agents were investigated. The developed films were characterized for the changes of physical, chemical, mechanical and biological properties comparing with the unmodified BC film. MBAG refers to BAG containing plasticizer; MBAGT refers to MBAG containing tannic acid and MBAGTM refers to MBAGT containing the mangosteen ethanolic extract.

4.1 Bioactive compounds in mangosteen ethanolic extract

In this study, mangosteen ethanolic extract was applied as natural antimicrobial agent. The crude extracts were analyzed by UV-Vis spectroscopic technique for determining the contents of bioactive compounds consisting in those extracts. Phenolic compounds were expressed by gallic acid equivalents (GAE) and mangostins were revealed by α-mangostin equivalents (AME). The contents of bioactive compounds in mangosteen ethanolic extract were shown in Table 4.1. The crude mangosteen ethanolic extract was composed of phenolic compound and mangostins at 0.45±0.02 mg GAE/ mL extract and 366.69±0.04 mg AME/ mL extract, respectively. The mangostins, which are the major compounds in mangosteen ethanolic extract, are typically hydrophobic components (Nguyen and Marquis, 2011).

Table 4.1 The contents of bioactive compounds in mangosteen ethanolic extract

Mangosteen Ethanolic Extract (ME)	Bioactive compounds	Amount of bioactive compounds (mg) in mangosteen ethanolic (per 1 mL) extracts
Conc. ME	Phenolic compound	0.44
	Mangostins	366.69
1% v/v of ME	Phenolic compound	N/A
	Mangostins	5.93
5% v/v of ME	Phenolic compound	N/A
	Mangostins	11.72
10% v/v of ME	Phenolic compound	N/A
	Mangostins	22.80

4.2 Characterization of BAG films and modified BAG films by plasticizer (MBAG films)

4.2.1 Transparency

In Figure 4.1, the alphabets beneath the films show the transparency of the films. The film thickness was around 0.05 mm. Films of BC, sodium alginate and BC/A at a ratio of 60/40 was slightly opaque, whereas a film of gelatin was more transparent. Transparency of the films was increased with increasing gelatin content. It was found that the BAG film at a ratio of 60/10/30 was a highly transparent film. The surface roughness and film thickness might also affect transparency of films (Park et al., 2008). However, no significant difference in the degree of transparency was observed between the films with and without the addition of glycerol, sorbitol and the mixture of glycerol and sorbitol as shown in Figure 4.2.

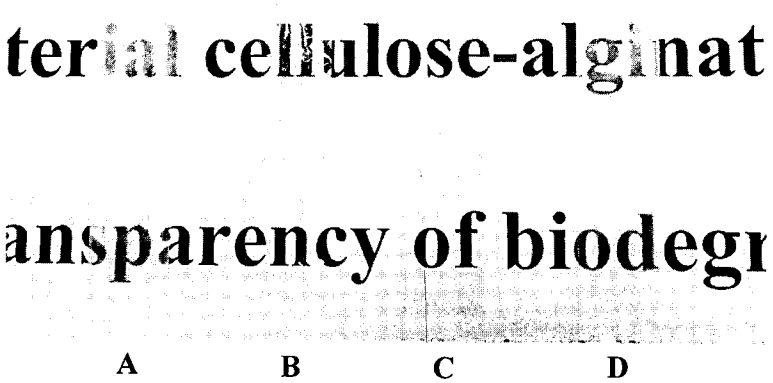

Figure 4.1 Transparency of films: bacterial cellulose (A), sodium alginate (B), gelatin (C) and BC/A at a ratio of 60/40 (D)

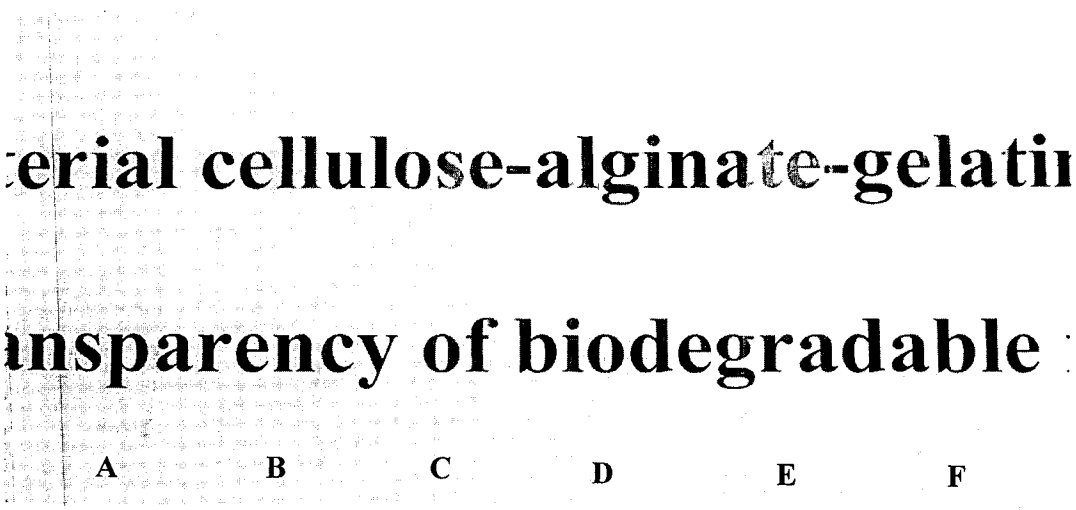

Figure 4.2 Transparency of films: the BAG films at a ratio of 60/10/30 (A), 60/20/20 (B) and 60/30/10 (C), and the MBAG films at a ratio of 60/20/20 with glycerol (D), sorbitol (E), the mixture of glycerol and sorbitol (F)

4.2.2 Fourier transforms infrared spectroscopy (FT-IR)

The FT-IR spectra of BC, sodium alginate, gelatin, BC/A and the BAG films without and with plasticizer adding at a ratio of 60/10/30, 60/20/20 and 60/30/10 were determined with the wavenumber ranging from 4000 to 400 cm^{-1} as shown in Figure 4.3 and 4.4.

Figure 4.3 exhibits the main functional groups of each pure key component. The three main peaks of BC were C-O-C and O-H stretching vibration at 1061and 3392 cm^{-1}, and H-O-H bending vibration of absorbed water molecules consisting in the structure of BC at 1647 cm^{-1}. The five main peaks of alginate were C-O-C at 1035 cm^{-1}, overlapping O-H and N-H at 3411 cm^{-1}, the ester group (-COO) stretching vibration at 1423 cm^{-1} and H-O-H bending vibration of absorbed water molecules consisting in the structure of sodium alginate at 1607 cm^{-1} which it also can be assigned to C=O stretching (Lojewska et al., 2005). Additionally, the characteristic absorption bands of sodium alginate appeared around 820 cm^{-1} (Xiao et al., 2001). The four main peaks of gelatin were the N-H stretching of amide at 3408 cm^{-1} due to the extension of the group. The intense bands of the peptide groups at 1643 and 1543 cm^{-1}as bands of amide I (extension of C=O) and amide II (extension of C–N and angular deformation of the N–H ligation), respectively. Amide III, with bands at 1239 cm^{-1}, represents components of the extension of C-N and N-H on the flexion surface of amide bonds and absorptions as a result of the vibrations of groups C–H_2 of the glycine and proline (Sionkowska et al., 2004; Andreuccetti et al., 2009). The last one, the BC/A at a ratio of 60/40 shows main five peaks as the C-O-C and the O-H stretching vibration at 1026 and 3392 cm^{-1}, the H-O-H bending vibration of absorbed water molecules consisting in the structure of BC, at 1611 cm^{-1}, the ester group (-COO) at 1424 cm^{-1} and the characteristic absorption bands of sodium alginate and 819 cm^{-1}.

The FT-IR spectra of BAG films at ratios of 60/10/30, 60/20/20 and 60/30/10 without plasticizers and at ratios of 60/20/20 with plasticizers exhibit the characteristic absorption bands with no appearance of new peaks as shown in Figure 4.4 A to F. The BAG films at ratio of 60/10/30, 60/20/20 and 60/30/10 appeared peaks of main functional groups. The C-O-C stretching vibration of BC and alginate

is observed at about 1026-1059 cm^{-1}, the O-H and N-H stretching vibration at about 3400-3404 cm^{-1}, the H-O-H bending vibration of absorbed water molecules consisting in the structure of BC appeared at about 1613-1650 cm^{-1} which it also can be assigned to the C=O stretching. The ester group stretching vibration (-COO) of alginate appeared at 1423-1424 cm^{-1}. The symmetric of N-H bending vibration in amide of gelatin appeared at 1535 cm^{-1}, and the C-N stretching bands appeared at about 1241-1316 cm^{-1} of gelatin.

For the films at ratios of 60/20/20 with glycerol, sorbitol and the mixture of glycerol and sorbitol (GS) adding, multiple shifted bands were observed as follows. The C-O-C stretching bands were shifted to 1060, 1035 and 1059 cm^{-1}, and the O-H and the N-H stretching bands were shifted to 3401, 3400 and 3393 cm^{-1}, respectively. The H-O-H bending peaks were shifted to 1650, 1635 and 1649 cm^{-1} and the -COO stretching peaks were shifted to 1431, 1424 and 1431 cm^{-1}, respectively. The symmetric of N-H bending peaks were shifted to 1535, no peak and 1541 cm^{-1} and the C-N stretching peaks were shifted to 1243, 1250 and 1243 cm^{-1}, respectively.

It was shown that the MBAG films with glycerol adding tended to increase in amplitudes of the gelatin characteristic absorption band and free water peaks (Bergo and Sobral, 2007). The C=O stretching was shifted to higher frequency at 1650 cm^{-1} and appeared N-H bending vibration of at 1535 cm^{-1}. The FT-IR peaks of the MBAG films with sorbitol adding tended to increase in amplitudes of the sodium alginate characteristic absorption band. These shifts could be attributed to intermolecular interactions between the hydroxyl group of cellulose, the carboxyl group of sodium alginate and amide group of gelatin.

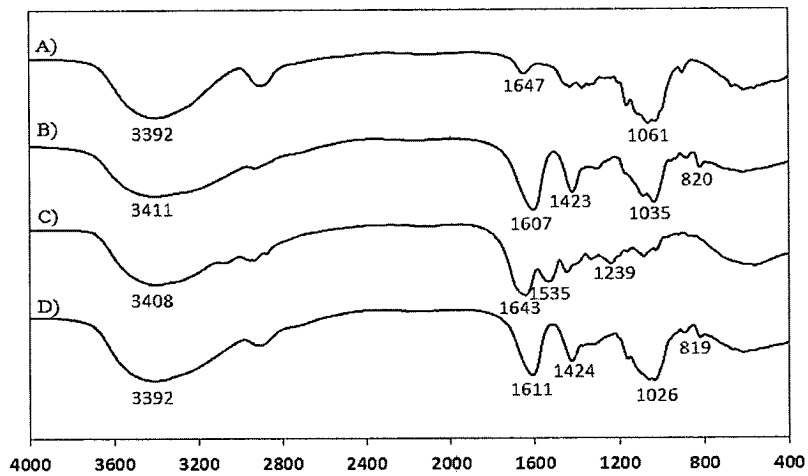

Figure 4.3 FT-IR of films at a ratio of BC (A), Sodium alginate (B), Gelatin (C) and BC/A film (D)

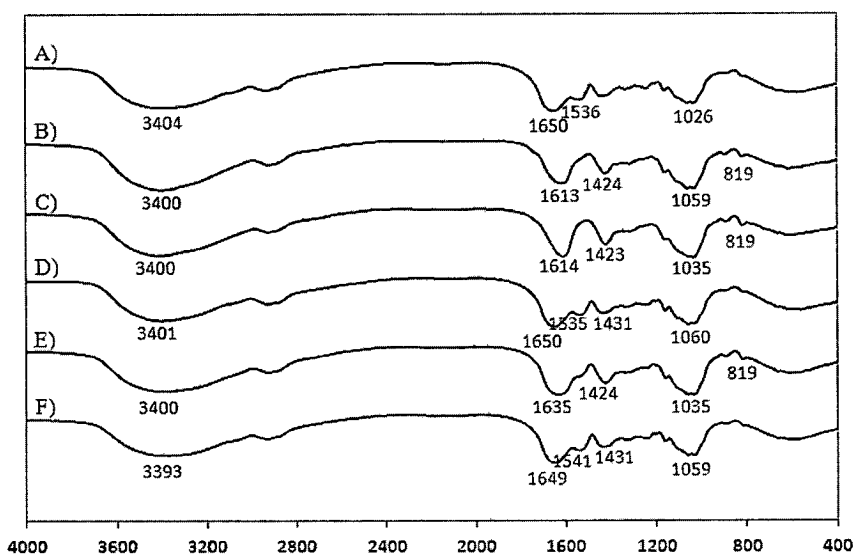

Figure 4.4 FT-IR of BAG films at a ratio of 60/10/30 (A), 60/20/20 (B), 60/30/10 (C) and films at a ratio of 60/20/20 with glycerol (D), sorbitol (E) and the mixture of glycerol and sorbitol (F) addition, respectively.

4.2.3 Water absorption capacity (WAC)

The WAC of the films in DI water is shown in Figure 4.5 and 4.6. The results indicated that the WAC values were correlated with the gelatin content. The WAC of BC, sodium alginate and BC/A was 254.4, 296.8 and 208.7%, respectively, whereas the BAG films at a ratio of 60/10/30, 60/20/20 and 60/30/10 was 411.9, 344.5 and 232.5%, respectively. The increased WAC of the BAG films at a ratio of 60/10/30 was due to very hydrophilic nature and more flexible structure of gelatin. Similar observations were previously reported in modified BC by BC/gelatin composites via cross-linking (Chang et al., 2012).

The addition of plasticizer into the BAG films up to certain amount enhanced WAC of the BAG films. The results indicated that WAC increased with the increase of plasticizer content. However, excess of plasticizer at a ratio of plasticizer to gelatin solution more than 2:10 (w/w) caused the decrease of the WAC, which should be due to the migration of plasticizer from the re-swollen film surface. Similar observations were previously reported in DCMC crosslinked gelatin edible film (Mu et al., 2012). The plasticized films at a ratio of plasticizer to gelatin solution at 2:10 (w/w) showed better rehydration ability and water absorption capacity.

For the effect of type of plasticizers, WAC of the films plasticized with sorbitol (S) had a greater WAC than that plasticized with the mixture of glycerol and sorbitol (GS) and glycerol (Gly), respectively. Because sorbitol is polyol containing multiple hydroxyl groups in the structure, it could attract with -OH of water molecules.

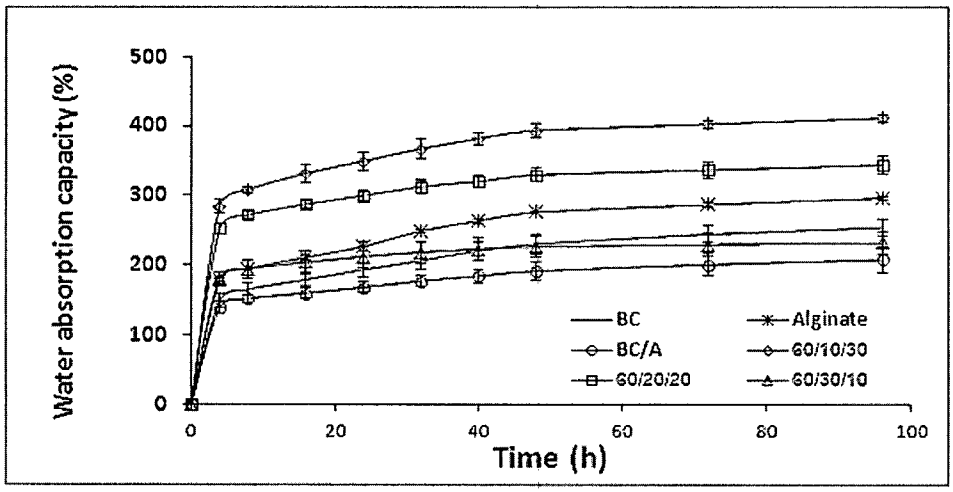

Figure 4.5 Water absorption capacity (%) of the composite films: BC (—); Alginate (—✳—); BC/A (—◇—); BAG films at a ratio of 60/10/30 (—◇—), 60/20/20 (—□—) and 60/30/10 (—△—) without plasticizer, respectively.

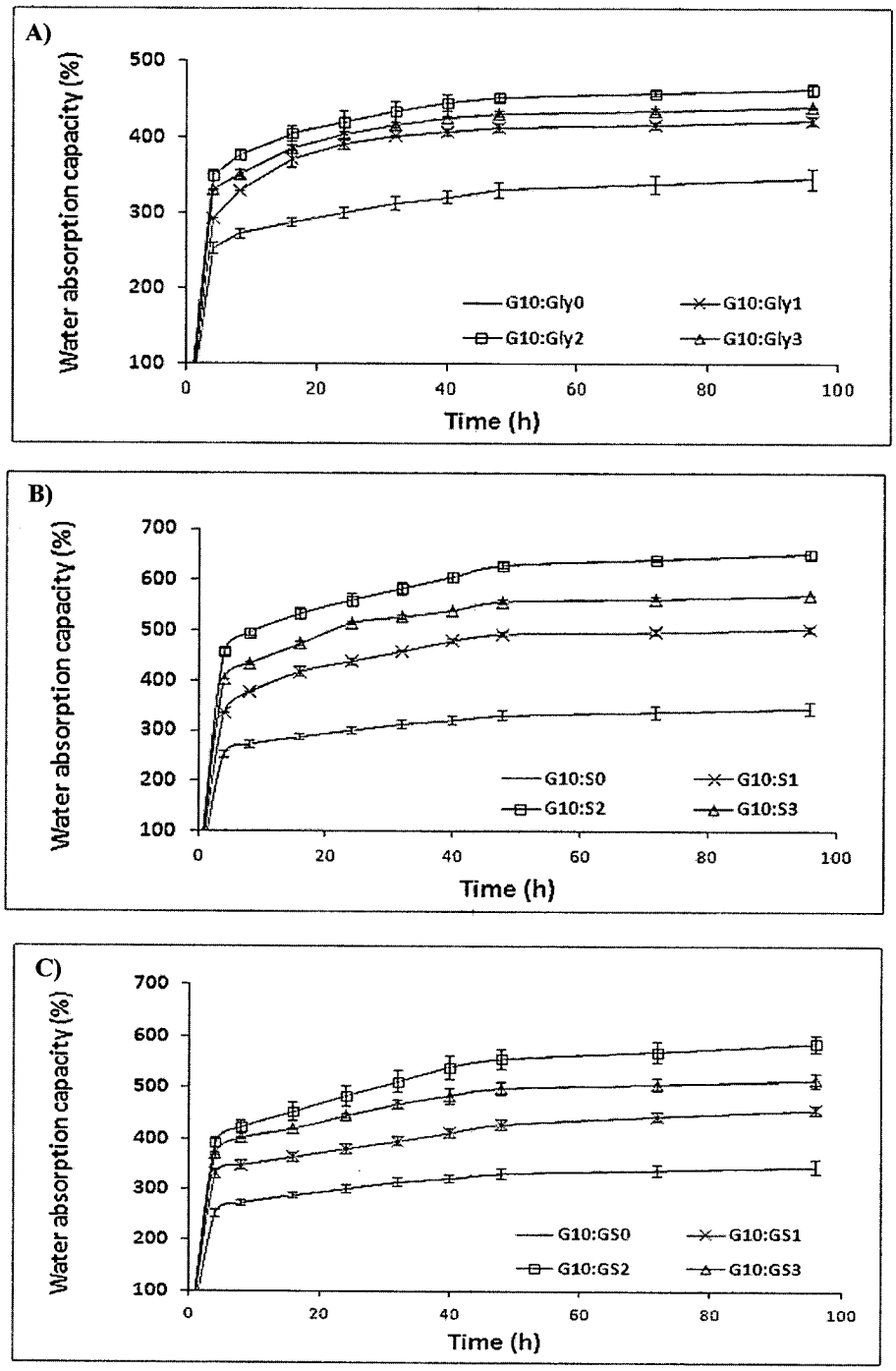

Figure 4.6 Water absorption capacity (%) of the composite films: films at a ratio of 60/20/20 with glycerol (A), sorbitol (B) and the mixture of glycerol and sorbitol (C); G:Gly, G:S and G:GS refer to a ratio of gelatin to glycerol, sorbitol and the mixture of glycerol and sorbitol (w/w), respectively.

4.2.4 Mechanical properties

Tensile strength (TS) and elongation at break (EB) of the homogenized BC, sodium alginate and BAG films in dry state were shown in Figure 4.7 A and B. The TS and EB of the BC film were 57.5 MPa and 1.0%, whereas those of the BC/A films were 147.9 MP and 2.1%, respectively. For TS and EB of the BAG films without plasticizer at ratios of 60/10/30, 60/20/20 and 60/30/10 were 166.5, 181.8 and 177.5 MPa, and 2.0, 2.9 and 2.0%, respectively. And the TS and EB of BAG films in dry state in different ratios of each plasticizer were shown in Figure 4.8 A and B.

Overall, the films at a ratio of 60/20/20 (w/w) showed superior mechanical properties in dry state; the TS and EB were at 181.8 and 2.9%, respectively. Moreover, the results showed that there was no significant difference between the mechanical properties of the dried films with and without addition of glycerol as plasticizer. The function of plasticizer is to enhance the flexibility and plasticity to the films but it might not affect some functional properties (Vanin et al., 2005).

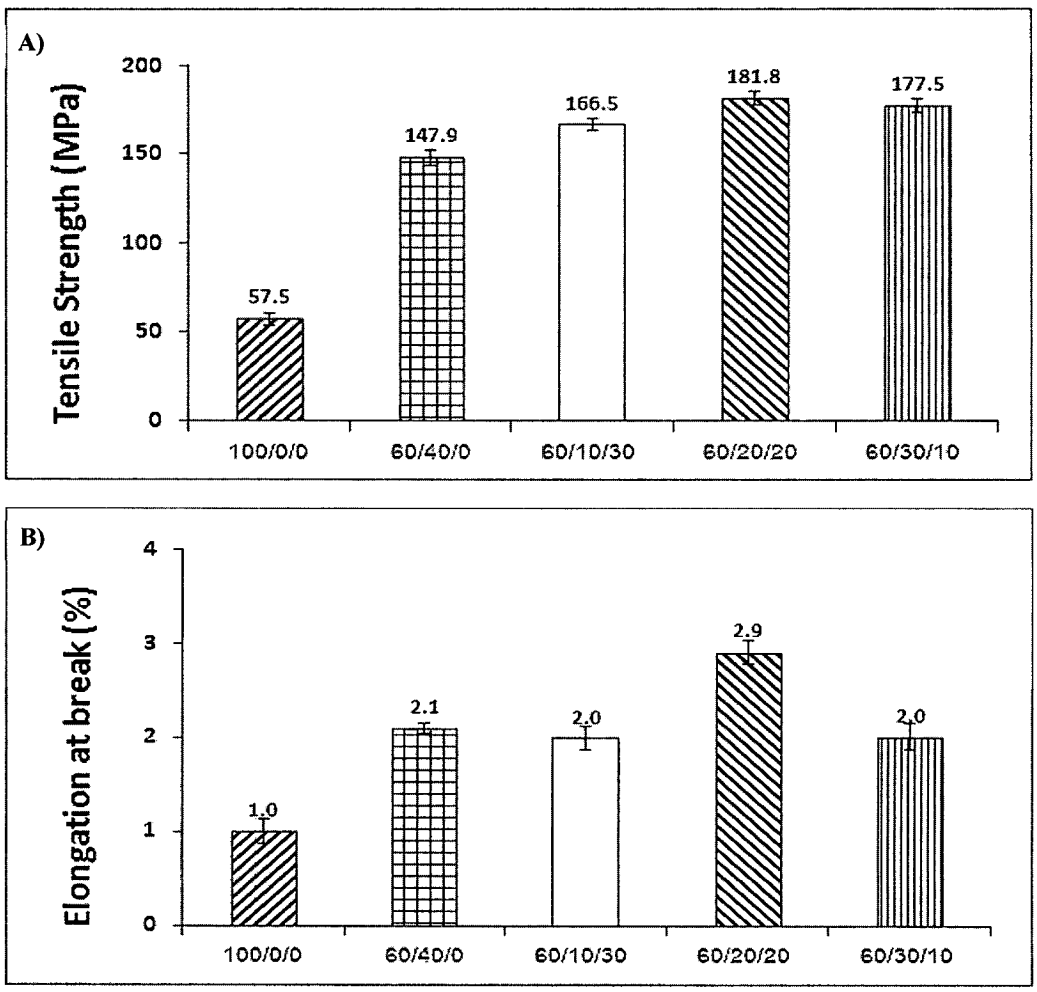

Figure 4.7 Mechanical properties of BAG films in dry state without plasticizer addition: Tensile strength (A) and Elongation at break (B).

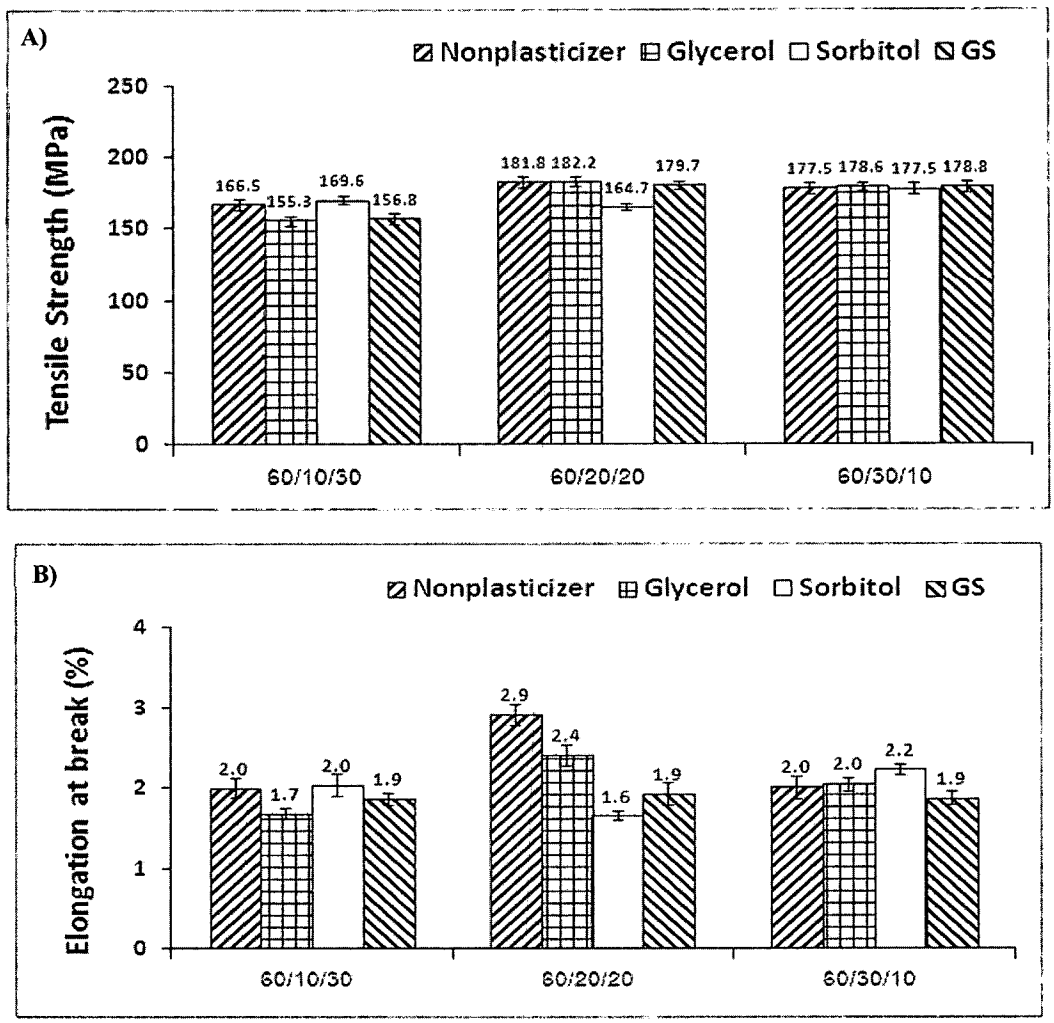

Figure 4.8 Mechanical properties of BAG films in dry state without and with plasticizer addition: Tensile strength (A) and Elongation at break (B).

Tensile strength (TS) and elongation at break (EB) of the homogenized BC, alginate and BAG films in wet state were shown in Figure 4.9 A and B. The TS and EB of the BC film were 2.2 MPa and 1.9%, whereas those of the BC/A films were 15.3 MP and 18.0%, respectively. For TS and EB of the BAG films without plasticizer at ratios of 60/10/30, 60/20/20 and 60/30/10 were 2.3, 9.6 and 11.3 MPa, and 14.8, 30.3 and 28.0%, respectively. And the TS and EB of BAG films in wet state in different ratio of each plasticizer were shown in Figure 4.10 A and B.

Overall, the films at a ratio of 60/30/10 (w/w) showed superior mechanical properties in wet state; the TS and EB were 9.6 MPa and 30.3%, respectively. It was shown that TS and EB of the MBAG film with glycerol were more stable with higher TS and EB than the others. Since both gelatin, glycerol and sorbitol are hydrophilic and high flexible components, significantly improved EB of the BAG films in re-swollen form with the addition of glycerol, sorbitol and the mixture of glycerol and sorbitol (GS) as plasticizer was observed. For the MBAG film at ratios of 60/10/30, 60/20/20 and 60/30/10 with glycerol adding as plasticizer, the EB increased to 22.9, 44.6 and 45.7%, respectively.

It was found that TS of the re-swollen BAG films was reduced with the addition of plasticizer. In the wet state, the TS of the BAG films plasticized with glycerol was more than that plasticized with GS and S, respectively. Overall, gelatin and glycerol helped to improve high flexibility and lowered TS of the BAG films in the wet state. It was previously reported that the addition of glycerol to gellan films increased extensibility, but reduced the mechanical strength (Yang and Paulson, 2000) and the softness and flexibility of gelatin-based films could be improved by the addition of plasticizers.

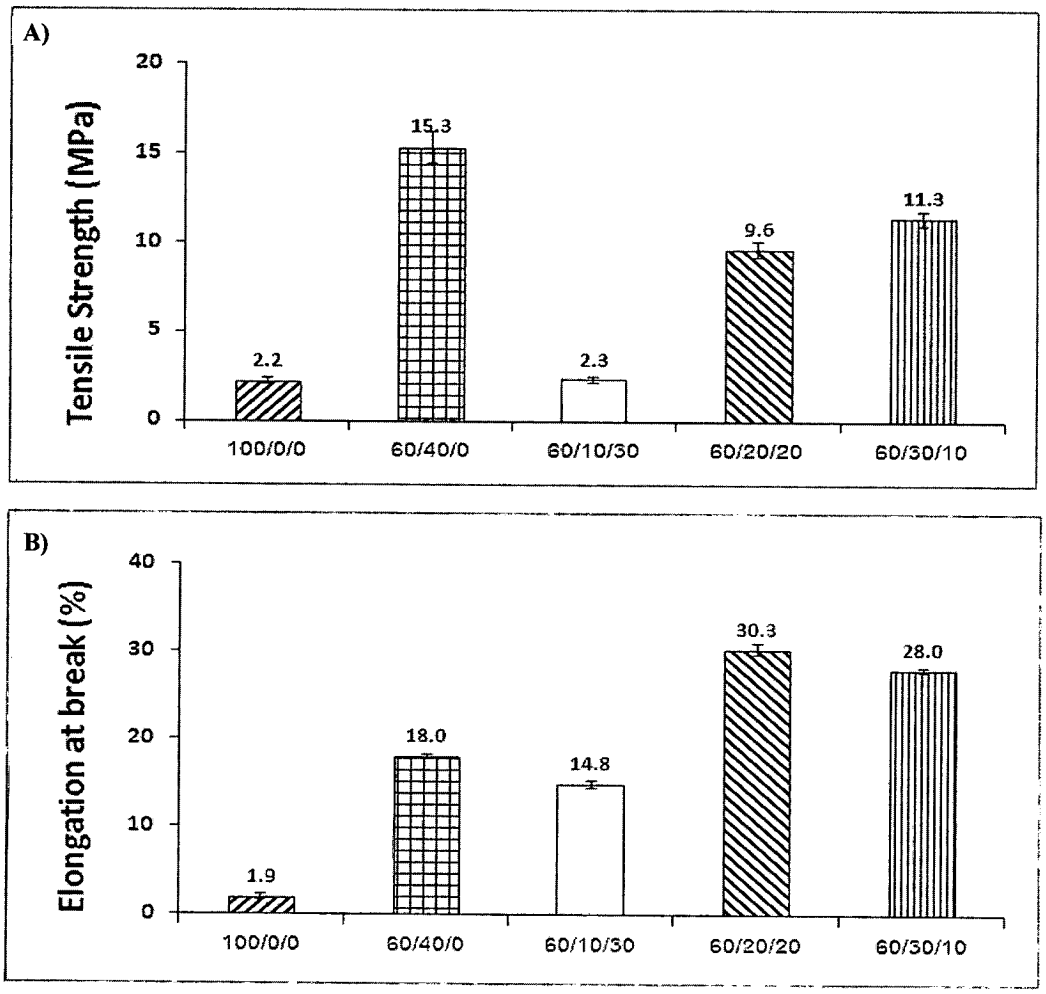

Figure 4.9 Mechanical properties of BAG films in wet state without plasticizer addition: Tensile strength (A) and Elongation at break (B).

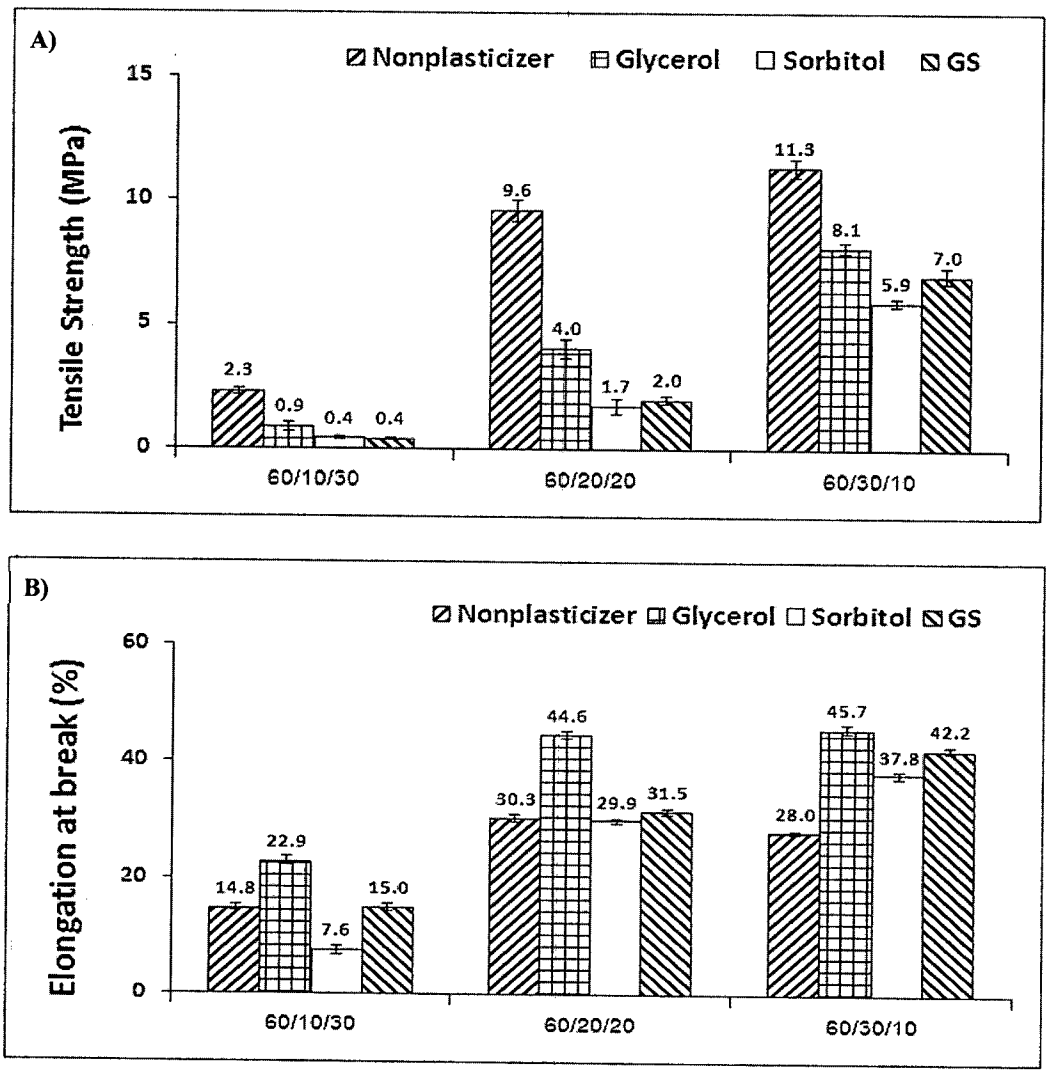

Figure 4.10 Mechanical properties of BAG films in wet state without and with plasticizer addition: Tensile strength (A) and Elongation at break (B).

4.2.5 Scanning electron microscope (SEM)

SEM images of overview surface morphology at 200 magnifications of the films in dry state were shown in Figure 4.11 (A-H). The surface roughness of BC film has been shown in Figure 4.11 (A) due to cellulose fibrils. Sodium alginate and gelatin films have smooth surfaces. Under the cross linking with $CaCl_2$, the alginate film formed wavy surface pattern. BC/A and BAG films also exhibited surface roughness from cellulose fibrils.

SEM photographs revealed surface morphology at 10,000 magnifications of the BAG films at different ratio are shown in Figure 4.12 (A-F) and the MBAG films in dry and wet state at a ratio of 60/20/20 plasticized with glycerol in Figure 4.12 (G and H). From the SEM photograph exhibited that sodium alginate and gelatin lodged in BAG networks and wrapped up parts of the BC fibril network. Sodium alginate-gelatin-embedded BC formed a film on which only several enlarged cellulose ribbons were observed. Moreover, sodium alginate and gelatin became the continuous phase and formed a more massive film when BC was blended with both ones. A substantial amount of sodium alginate and gelatin not only filled the network but also embedded completely on cellulose ribbons. However, a few bigger holes still existed in the composites.

Compared to the dried films, the re-swollen films exhibited a looser fibril network structure according to the high water absorption of the films. The BAG film at a ratio of 60/10/30 found that it was looser structure than the film at other ratio and the film at a ratio of 60/30/10 found that it was not clearly observed of cellulose ribbon because a lot of sodium alginate content increased thickener in the film affect well wrap cellulose ribbon and the structure of the film became less uniform with noticeable excessive alginate on the film surfaces. For the film at a ratio of 60/20/20 displayed good incorporation of sodium alginate and gelatin into the BC fibril network because the structure its ordered cellulose ribbon rather.

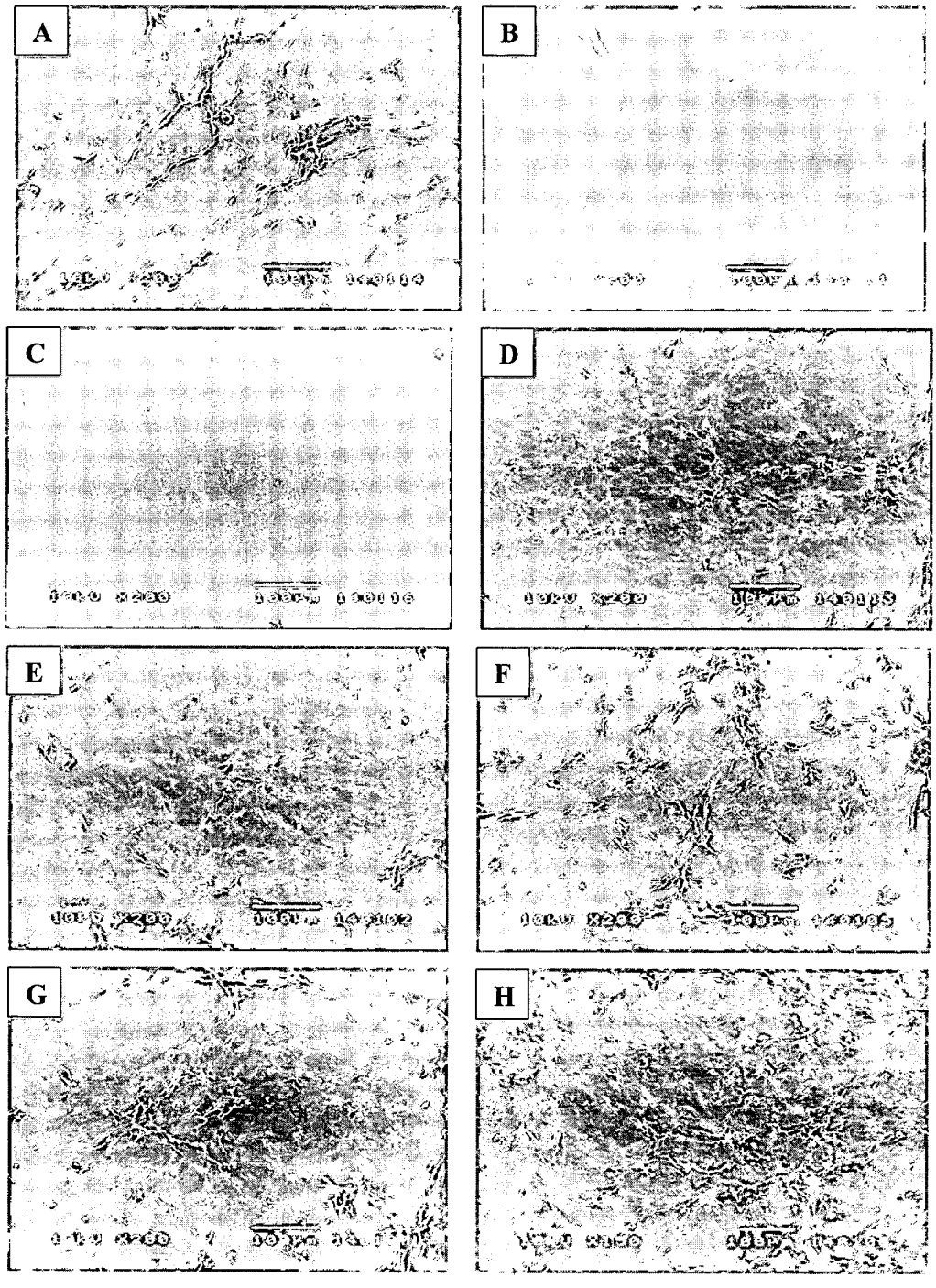

Figure 4.11 SEM images of overview surface morphology of the films in dry state: BC (A); Sodium alginate (B); Gelatin (C); BC/A (D); BAG films at a ratio of 60/10/30 (E), 60/20/20 (F), 60/30/10 (G) and MBAG film at a ratio of 60/20/20 plasticized with glycerol (H).

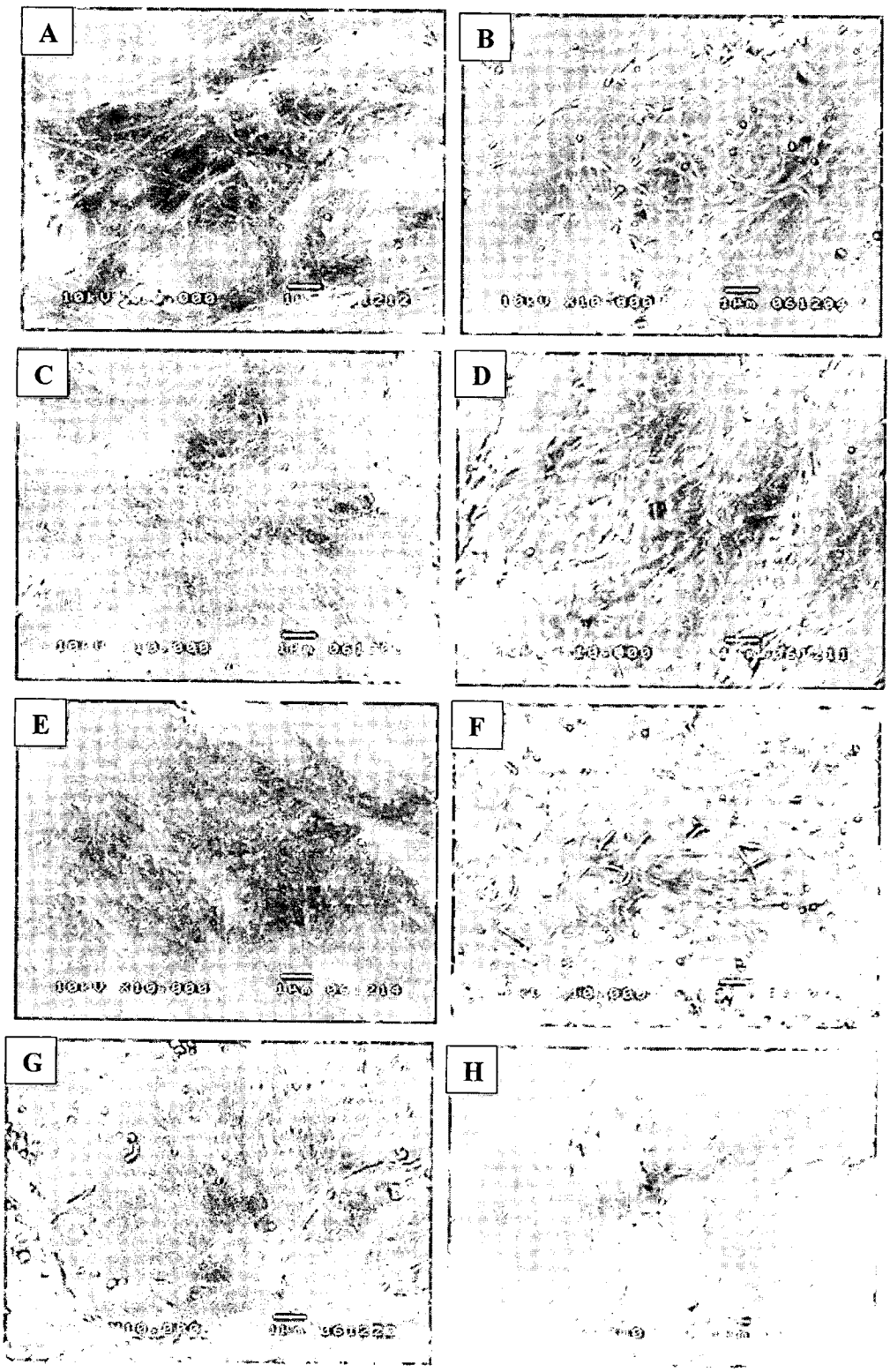

Figure 4.12 SEM images of surface morphology of BAG films in dry (left) and re-swollen (right) forms at a ratio of 60/10/30 (A and B), 60/20/20 (C and D), 60/30/10 (E and F) and MBAG film at a ratio of 60/20/20 plasticized with glycerol (G and H)

Figure 4.13 expressed the cross sectional morphologies of the BAG films at different ratio without glycerol (Figure 4.13 A-C) and the BAG film at a ratio of 60/20/20 with glycerol (Figure 4.13 D) at 3,500 magnifications. The images showed that the thickness of layer in the BAG films increased with the increase of sodium alginate content. However, the interlayer space between sheets was still observed. Moreover, gelatin could also penetrate into the fiber networks and partially filling in empty space between BC fibrils (Chang et al., 2012).

Moreover, in comparison with the native films, the addition of glycerol generated the looser BC fibril network as shown in Figure 4.12 (G, H) and Figure 4.13 (D). The result demonstrated that glycerol addition significantly increased void fraction of inter-chain in the BC fibril networks.

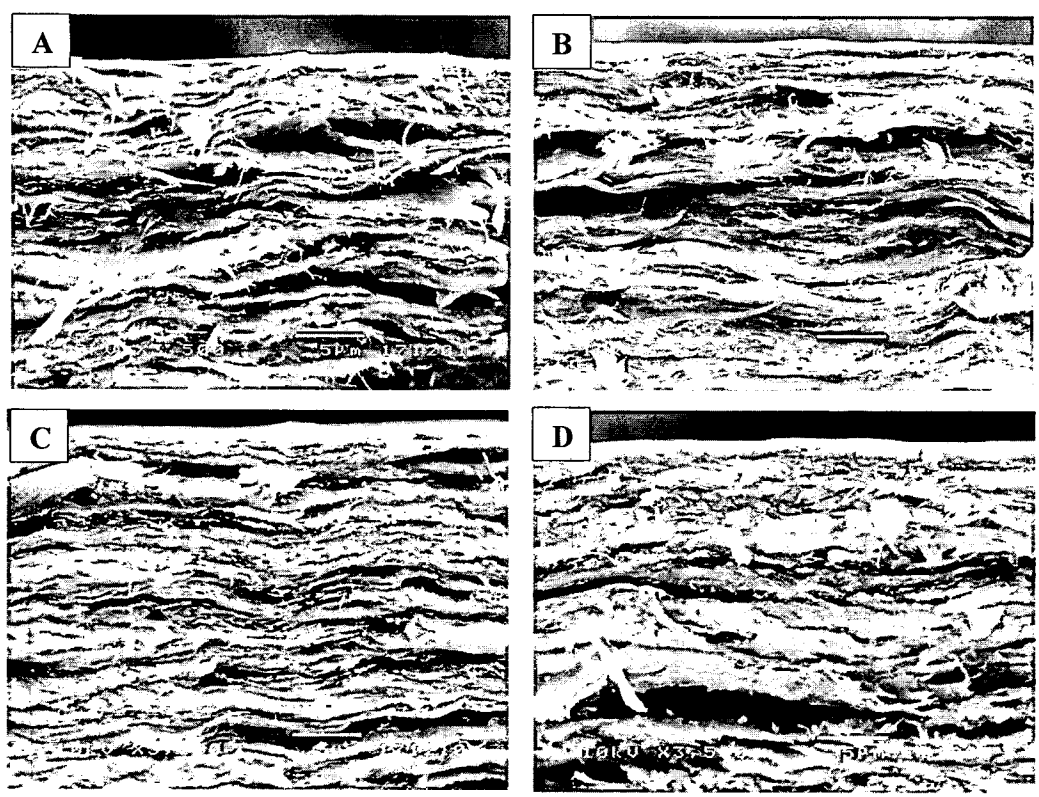

Figure 4.13 SEM images of cross-sectional morphology: BAG films in dry form at a ratio of 60/10/30 (A), 60/20/20 (B), 60/30/10 (C) and MBAG film at 60/20/20 plasticized with glycerol (D)

4.3 Characterization of MBAG films modified by tannic acid (MBAGT films)

4.3.1 Transparency

In Figure 4.14, the alphabets beneath the films show the transparency of the films. The film thickness was around 0.05 mm (50±10 μm). Transparencies of the films were relatively constant, not depending on tannic acid content. However, the tannic acid binding gelatin affected the color of the films. Since tannic acid could react with gelatin that is proteins, it caused the precipitation of tannic-proteins, which was responsible for the brownish color of the film.

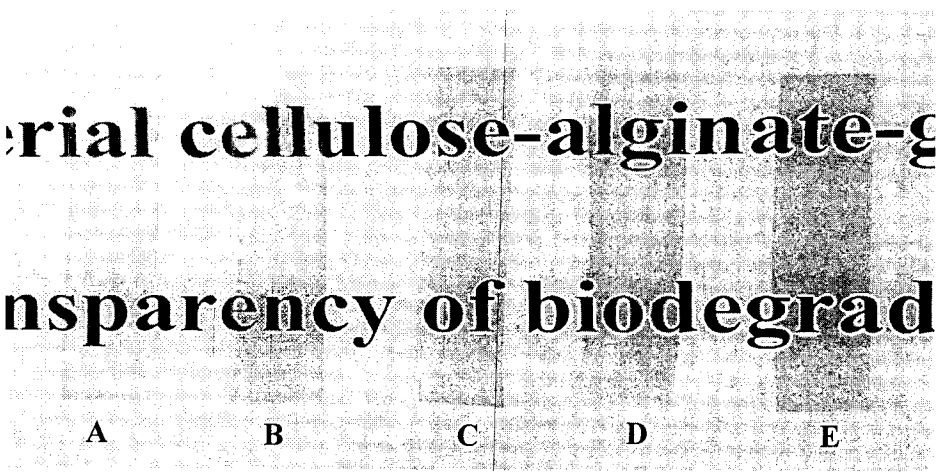

Figure 4.14 Transparency of films: the BAG films at a ratio of 60/20/20 without plasticizer (A), with glycerol (B), with glycerol and adding tannic acid at a ratio of 5 mg (C), 10 mg (D) and 15 mg (E) tannic acid per g gelatin solution, respectively

4.3.2 Fourier transforms infrared spectroscopy (FT-IR)

The FT-IR spectra of tannic acid, the BAG, MBAG, MBAGT films at a ratio of mg tannic acid to g gelatin as 5 mg, 10 mg and 15 mg are shown in Figure 4.15 A, B, C, D, E and F, respectively.

Generally, two broader peaks at around 1319 cm^{-1} and between 1290 and 1150 cm^{-1} (1200 cm^{-1}) can be observed in the spectra of gallic acid, tannic acid (gallotannin), and ellagitannin. Both peaks can be assigned to the combination of C-O stretching and -OH deformation vibrations (Edelmann and Lendl, 2002). The characteristic bands at 3408, 1615, and 1710 cm^{-1} represent phenolic hydroxyl group (-OH), double bond (C=C) in aromatic ring, and ester groups of phenolic compounds, respectively.

The BAG, MBAG and MBAGT exhibited the characteristic absorption bands with no appearance of new peaks. The BAG and MBAG films showed multiple bands that previously explained in Topic 4.1.2. For the MBAGT at the ratio of 5, 10 and 15 mg tannic acid to g gelatin solution, it was found that the C-O-C stretching peaks were shifted to 1060, 1059 and 1059 cm^{-1} and the O-H and the N-H stretching bands were shifted to 3413, 3412 and 3408 cm^{-1}, respectively. The H-O-H bending peaks were shifted to 1646, 1644 and 1650 cm^{-1}. The C=O stretching and the -COO stretching peaks were shifted to 1436, 1433 and 1443 cm^{-1}, respectively. The N-H bending peaks were shifted to 1541, 1536 and 1536 cm^{-1} and the C-N stretching peaks were shifted to 1236, 1236 and 1234 cm^{-1}, respectively.

Related to the content of tannic acid on MBAGT films, the results indicated that FT-IR peaks of the MBAGT films tended to increase in amplitudes of the H-O-H bending peaks or free water peaks at about 1646-1650 nm^{-1} and these changes were indicative of greater disorder in gelatin and were probably associated with the loss of triple helix state (Muyonga et al., 2004) Because tannic acid is high molecular weight hydrophilic highly compound, hydroxyl groups of tannin could either form hydrogen-bonded side-chain interactions or bind with carbonyl groups of gelatin molecules as indicated by additional the wavelength of -COO stretching peaks and H-O-H bending peaks group that were part of gallic acid unit in tannic found in MBAGT films.

Previously, these shifts could be attributed to the bending of the O-H bonds and the stretching of the C-O bonds in secondary and tertiary alcohols (Aewsiri et al., 2010).

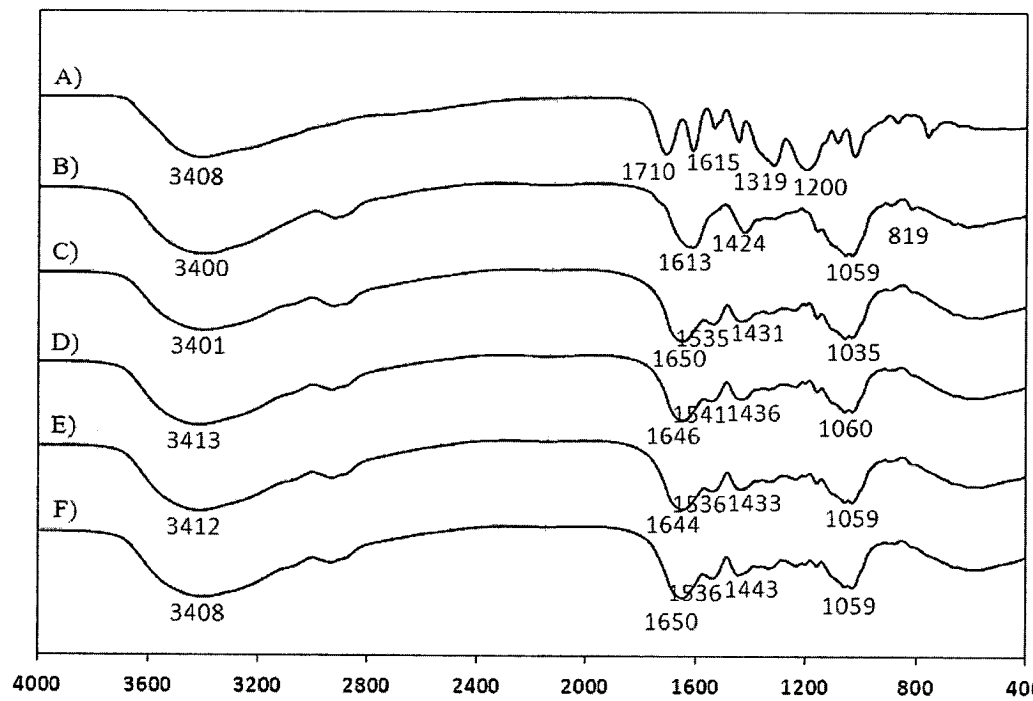

Figure 4.15 FT-IR of tannic acid (A), the BAG (B), MBAG (C), MBAGT at a ratio of mg tannic acid to g gelatin solution at 5.0 (D), 10.0 (E) and 15.0 (F) films.

4.3.3 Water absorption capacity (WAC)

The WAC of the MBAGT films in DI water is shown in Figure 4.16. The results indicated that the WAC values were inversely related with the tannic acid content. The WAC of the BAG film at a ratio of 60/20/20 and the MBAG film plasticized with glycerol adding (MBAG) was 333.6 and 462.2%. The WAC of the MBAG with tannic acid adding (MBAGT) at a ratio of 5, 10 and 15 mg tannic acid to g gelatin solution was 458.2, 389.9 and 345.6%, respectively. Similar observations were previously reported in modified gelatin film by tannin addition that it could repel enhancing water (Peña et al., 2010). Film-forming solution of gelatin cross-liked by tannic acid had effected to swelling ratio (Cao et al., 2007; Zhang et al., 2010).

For the addition of tannic acid as a crosslinking agent for gelatin, it was proposed that the increase of cross-linking degree resulted in the decrease of gelatin combination with water. Thus, the reduction in WAC values with increasing tannic content suggested the presence of interactions between tannic and gelatin. The rate of WAC is influenced by hydrophobic and/or hydrogen interactions between gelatin and tannic groups. The WAC rate decreased with the tannic acid content. In general, cross-linking and/or hydrogen interactions with other components decrease water uptake by proteins since polar-side-chain groups less exposed to bind water (Peña et al., 2010; Cao et al., 2007; Kim et al., 2005) and the more hydrophobic property from cross-linking with tannic acid, leading less water vapor absorption. In this work, the MBAGT film at a ratio of mg tannic acid to g gelatin solution at 10:1 was selected as it had high WAC and did not shrink or shrunk only slightly under the developed process.

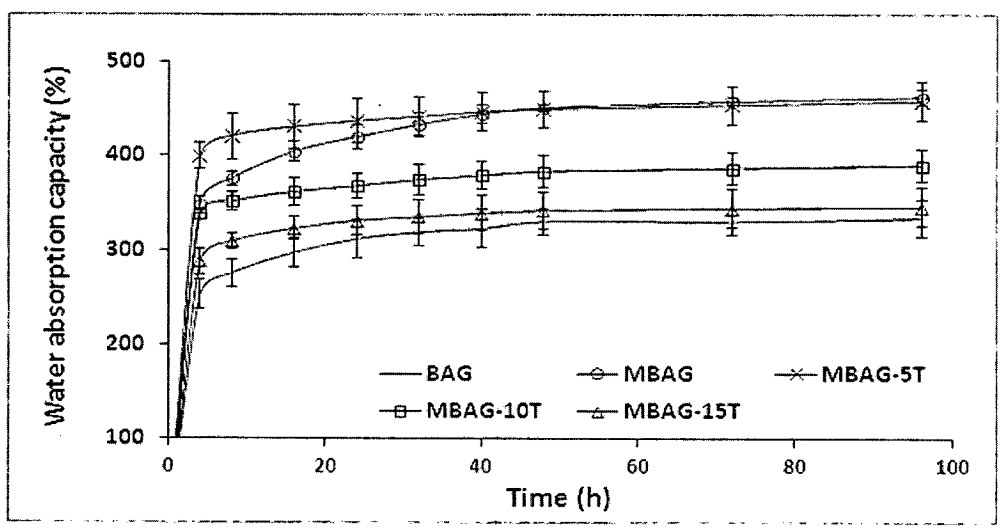

Figure 4.16 Water absorption capacity (%) of the composite films: BAG (—); MBAG (—○—); MBAG-5T (—×—); MBAG-10T (—□—) and MBAG-15T (—△—), respectively.

4.3.4 Mechanical properties

Tensile strength (TS) and elongation at break (EB) of the films of BAG, MBAG and MBAGT at a ratio of 5, 10 and 15 mg tannic acid to g gelatin solution in dry state are shown in Figure 4.17 A and B. The MBAGT films at a ratio of 5, 10 and 15 mg tannic acid to g gelatin solution exhibited slightly decreased mechanical properties from MBAG and BAG film to 174.8, 177.5 and 181.3 MPa, respectively. It could probably cause by some interfering of hydroxyl groups of tannic acid to the hydrogen bonding of cellulose. On the other hand, the hydrophobic interactions between tannic acid and gelatin contributed to the formation of complexes are considered far weaker than hydrogen bonding. However, at higher tannic acid content, the TS increased since the covalent cross-links between gelatin and tannin formed under high tannic acid concentration was more stable (Cao et al., 2007). Similar observations were previously reported in protein cross-linking with phenolic (Prodpran et al., 2012). According to the previous report (Zhang et al., 2010), tannic acid displayed a dual role as both a cross-linker (improving tensile strength) and plasticizer (improving elongation). However, no significant effect of tannic acid addition on plasticizer properties of the MBAGT films in dry state was observed. It was found that the EB of the MBAGT film slightly increased with the addition of 10 mg tannic acid/ g gelatin solution, but decreased with the addition of tannic acid at as 5 and 15 mg.

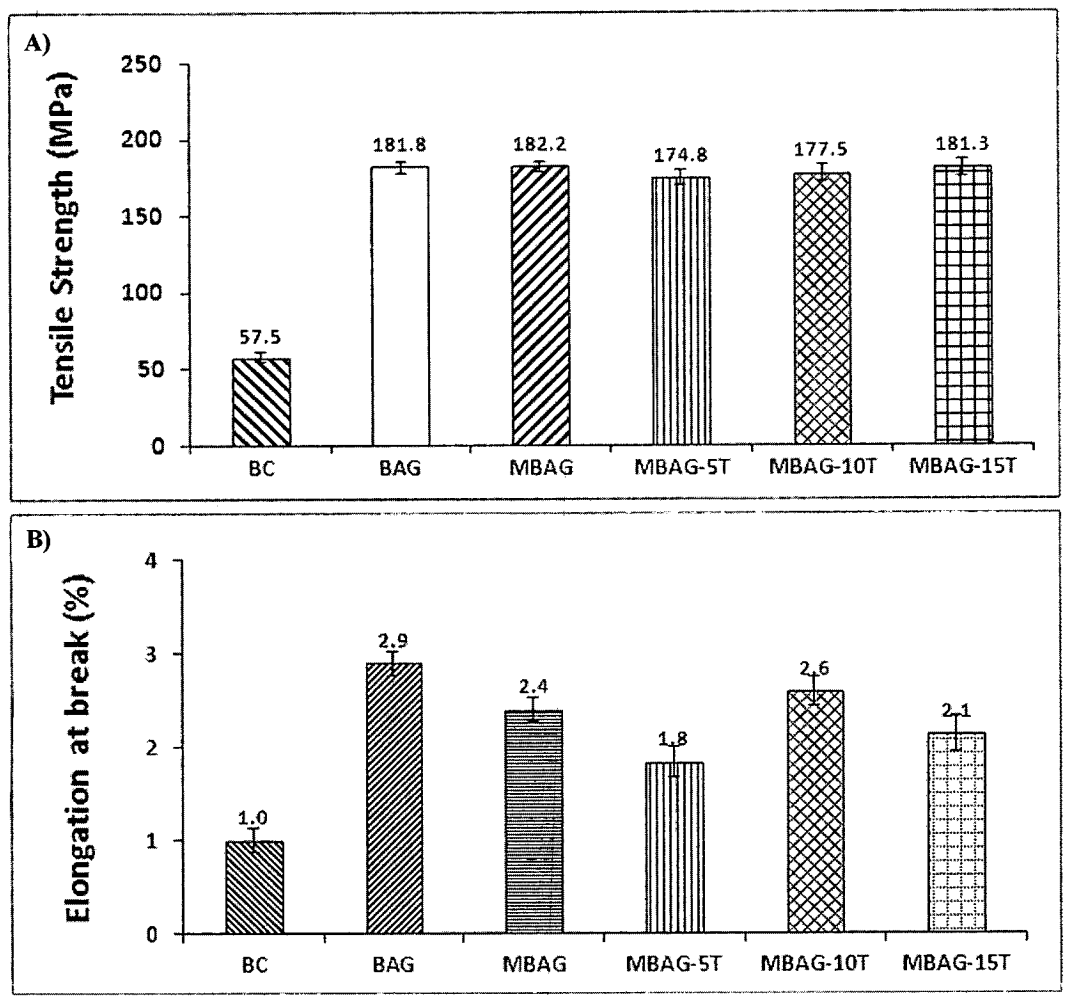

Figure 4.17 Mechanical properties of BAG films in dry state at a ratio of 5, 10 and 15 mg tannic acid to g gelatin solution (w/w): Tensile strength (A) and Elongation at break (B).

TS and EB of the films in wet state were shown in Figure 4.18 A and B. In wet state, the TS tended to decrease whereas EB tended to increase with the addition of tannic acid. The observations of the mechanical properties of the re-swollen films implied that the reactions between tannic acid and gelatin might be reversible.

Therefore, the interactions between tannic acid and gelatin in the MBAGT film should be hydrophobic interactions rather than strong hydrogen bonding. The reaction could reverse from tannic acid-gelatin precipitate to tannic acid-gelatin solution which similarly observation reported in tannin-protein interaction (Cao et al., 2007) as following:

Tannic acid solution + gelatin solution

↔ [Tannic acid m · gelatin] solution ↔ [Tannic acid n · gelatin] precipitate

Although the tannic acid-gelatin interaction was not strong, it had positive effect on plasticizer properties of MBAGT films in wet state and helped to increase EB of the re-swollen films.

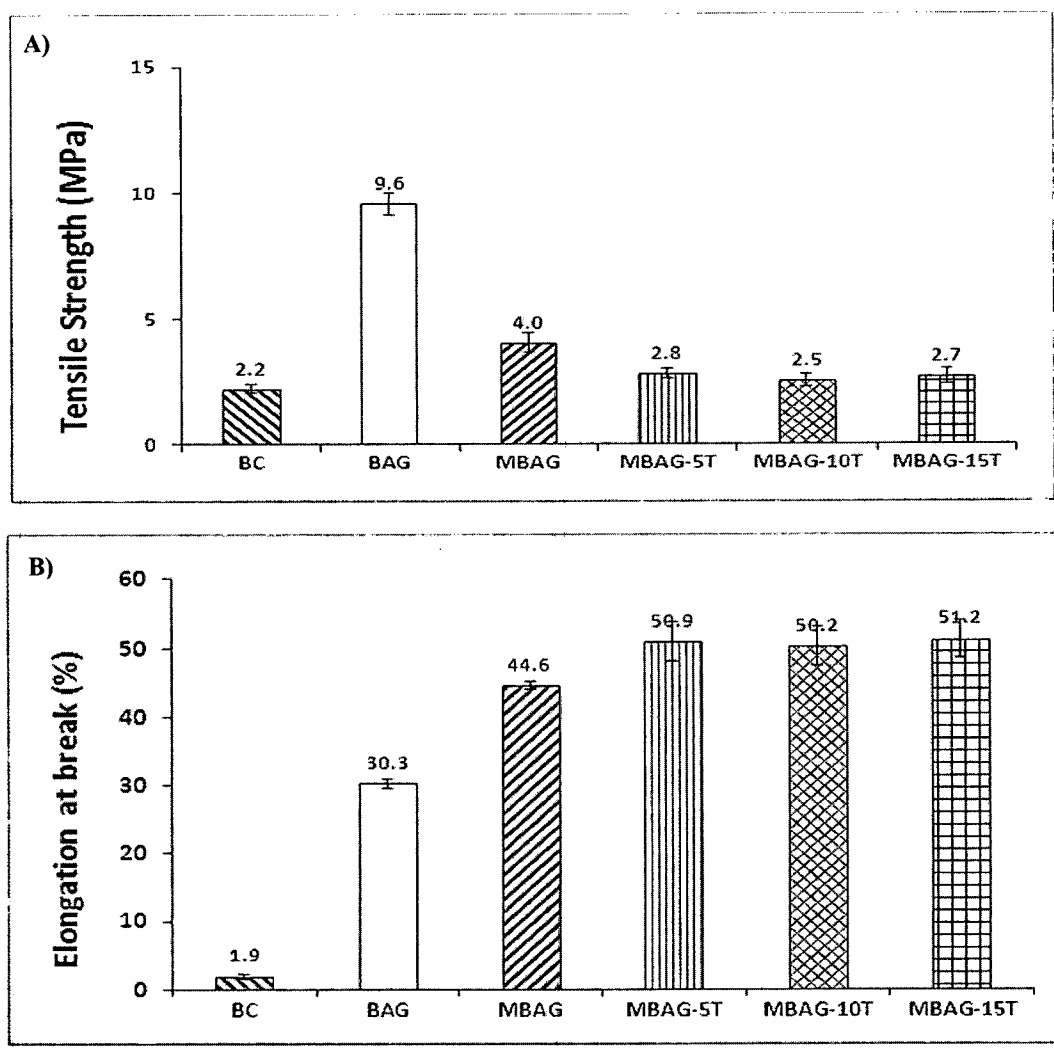

Figure 4.18 Mechanical properties of BAG films in wet state at a ratio of 5, 10 and 15 mg tannic acid to g gelatin solution (w/w): Tensile strength (A) and Elongation at break (B).

4.3.5 Scanning electron microscope (SEM)

SEM images of overview surface morphology of MBAGT films in dry state at 200 magnifications are shown in Figure 4.19 A, B and C. The surface roughness of MBAGT films due to cellulose fibrils distribution on surface was observed. It was noticed that the MBAGT film at a ratio of 10 mg and 15 mg tannic acid to g gelatin solution showed a smoother surface than that of 5 mg tannic acid content. It could probably suggest that the better tannic acid-gelatin interactions at higher tannic acid content might cause more precipitates covering the surface.

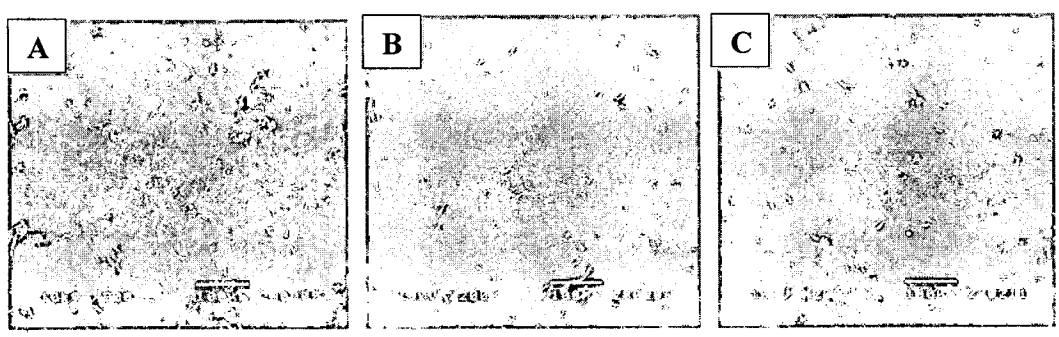

Figure 4.19 SEM images of overview surface morphology of MBAGT films in dry form at ratio of mg tannic acid to g gelatin solution (w/w): 5 mg (A); 10 mg (B); 15 mg (C).

SEM photographs revealed the surface morphology of the MBAGT films at 10,000 magnifications at a ratio of 5, 10 and 15 mg tannic acid to g gelatin solution are shown in Figure 4.20 (A-F), both in dry and wet states, respectively. The surface MBAGT films showed the formation of fibrils in gel and no significant difference in surface morphology was observed with the change of tannic acid content. The MBAGT films both in dry and re-swollen forms exhibited a dense structure without meso- and macropores. With the tannic acid cross-linked gelatin gels covering BC fibrils, the MBAGT films displayed better gel dispersion on cellulose fibrils as compared to MBAG films.

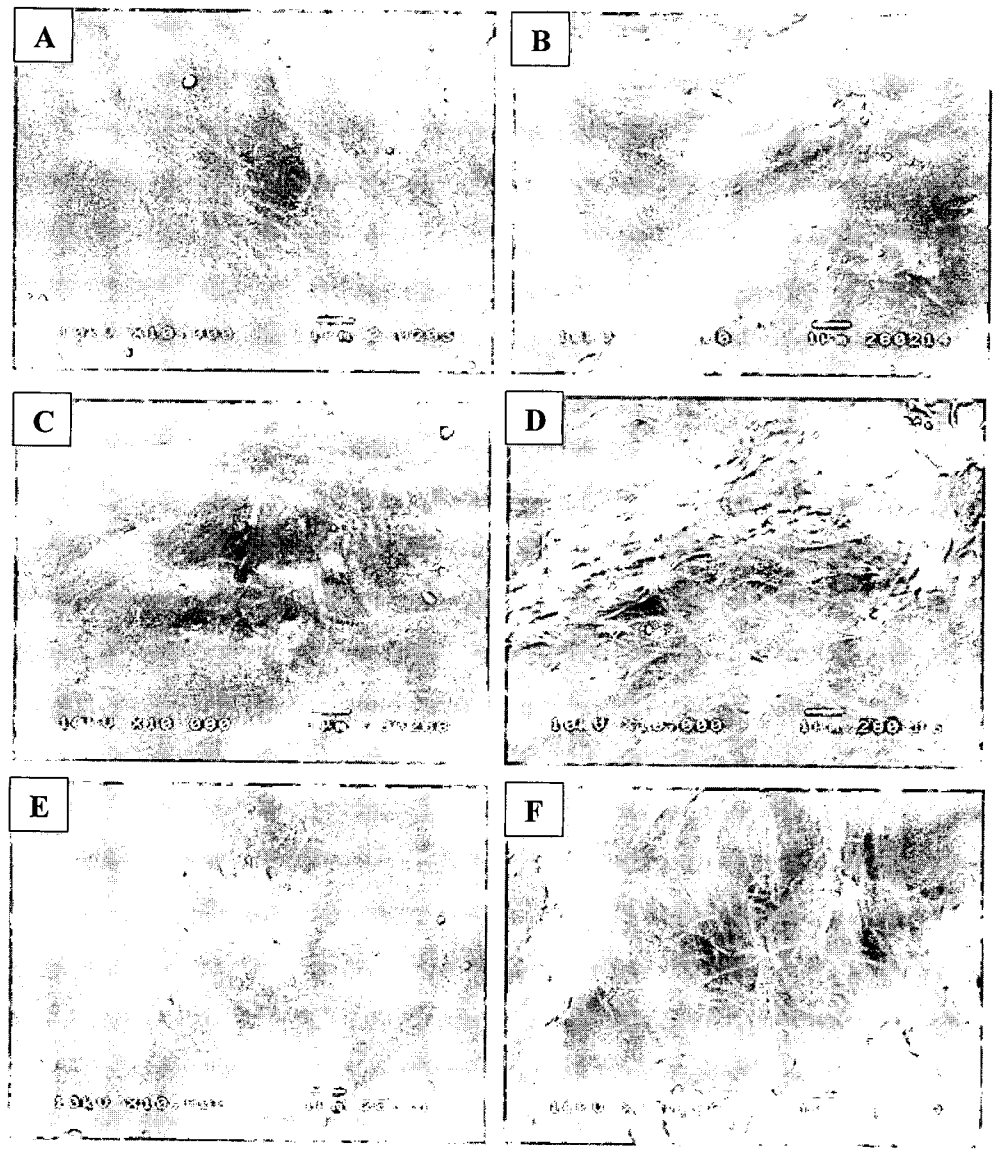

Figure 4.20 SEM images of surface morphology of MBAGT films in dry (left) and re-swollen (right) forms at a ratio of mg tannic acid to gram gelatin solution at 5 mg (A and B), 10 mg (C and D) and 15 mg (E and F).

Figure 4.21 expressed the cross sectional morphologies of the MBAGT films at different tannic acid content. The MBAGT films showed dense-packed sheet structure. However, no significant difference was observed with the change in tannic acid content. Compared to the MBAG films, the MBAGT films showed an apparent decrease in free volume of the packed sheet. Therefore, the cross-linking of gelatin by

tannic acid could reduce forced orientation relaxation. It was previously reported that with the use of tannic acid as a gelatin cross-linking agent, the alignment of the gelatin strand along the direction of deformation increased and the thickness of the layers, as well as the interlayer space decreased (De Carvalho and Grosso, 2004; Cao et al., 2007).

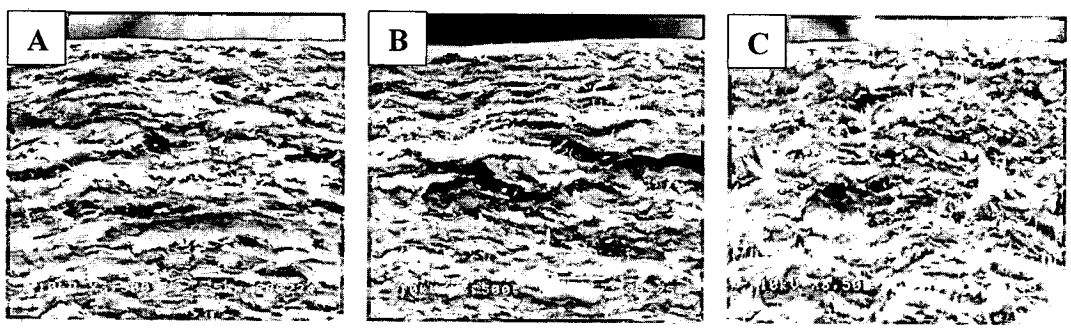

Figure 4.21 SEM images of cross sectional morphology: the MBAGT films in dry form at a ratio of 5 mg (A), 10 mg (B) and 15 mg (C) tannic acid to g gelatin solution.

4.4 Characterization of MBAGT films modified by mangosteen ethanolic extracts (MBAGTM films)

4.4.1 Transparency

In Figure 4.22, the alphabets beneath the films show the transparency of MBAGTM films. The film thickness was around 0.05 mm (50±10 μm). The MBAGTM film refers to the MBAGT film at a ratio of 60/20/20 which was modified for antimicrobial activities by adding the mangosteen extract. The MBAGTM films were more opaque as compared with the BAG, MBAG and MBAGT films. The transparency of the films decreased with the increase of mangosteen ethanolic extract from 1% to 5%. However, the increase of the mangosteen extract to 10% showed the relatively improved of film transparency compared to those with the lower mangosteen extract content. The color of the MBAGTM films changed from

brownish to yellowish brown color because the mangosteen ethanolic extract with tween 80 was yellowish brown in color.

The determination of the film transparency by using UV–visible spectrophotometer was shown in Figure 4.23. The result showed that the film transparency from high to low was in the following order: BAG > MBAG > MBAGT > MBAGTM10% > MBAGTM1% > MBAGTM5%.

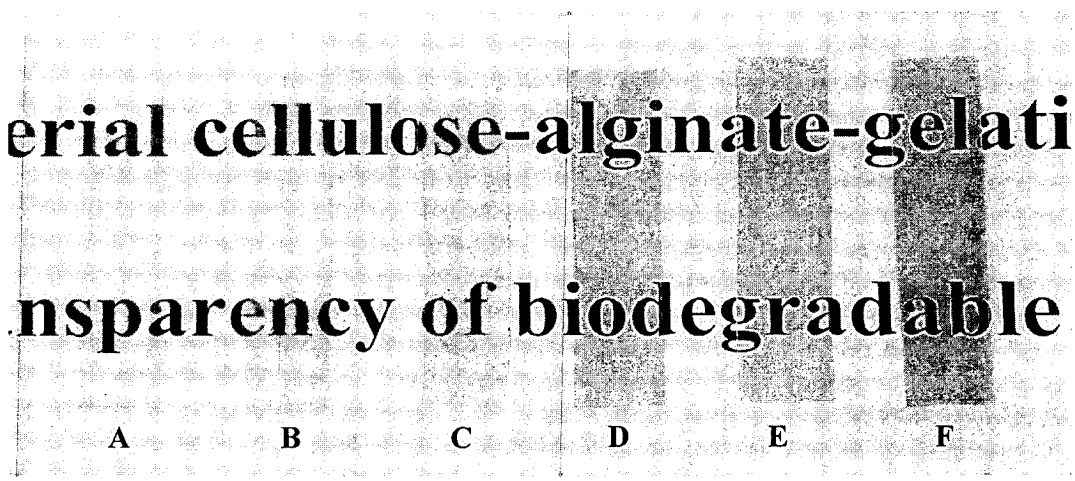

Figure 4.22 Transparency of films: the BAG films at a ratio of 60/20/20 without plasticizer (A), with glycerol (B), with glycerol and adding tannic acid at a ratio of 10 mg (C) tannic acid per g gelatin solution, with glycerol, tannic acid and the mangosteen ethanolic extract at concentration of 1% (D), 5% (E) and 10% (F) v/v, respectively.

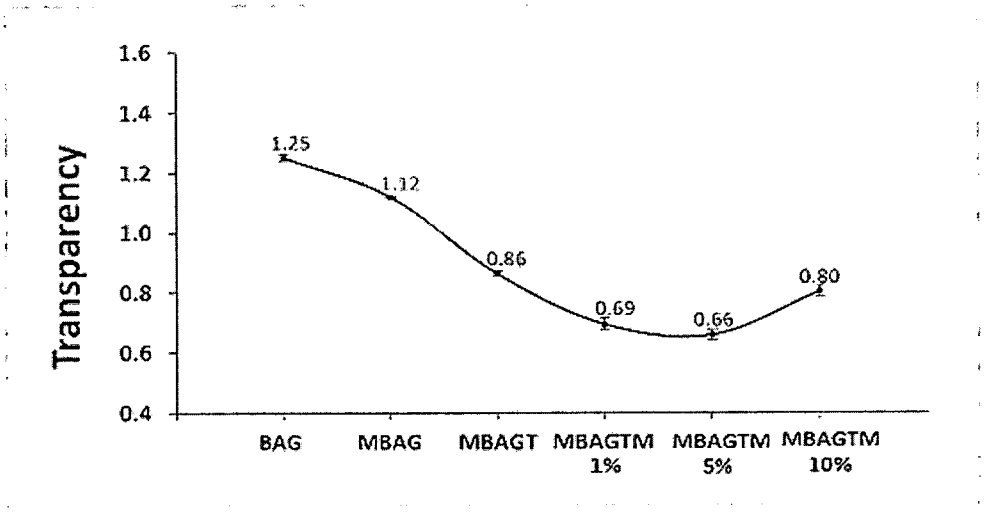

Figure 4.23 Transparency of films by using UV-visible spectrophotometer

4.4.2 Fourier transforms infrared spectroscopy (FT-IR)

The FT-IR spectra of mangosteen ethanolic extract, the BAG, MBAG, MBAGT and MBAGTM films at concentration of 1, 5 and 10% v/v mangosteen ethanolic extract are shown in Figure 4.24 A, B, C, D, E, F and G, respectively.

The characteristic absorptions of mangosteen extract are known to be associated with the stretching vibrations of C-H group stretching in aromatic ring of both aromatic and alkene at 2923 cm^{-1}, ether groups (C-O-C) and C-O (-C-OH) at 1108 cm^{-1}, ketone group (C=O) as chelate carbonyl group in the structure of xanthone backbone at 1736 cm^{-1} and phenolic hydroxyl group at 3370 cm^{-1}. The chelating of carbonyl group in the backbone of xanthone is shown in Figure 4.25. In particular, the band at 1108 cm^{-1} arises most probably from the C-O of aromatic -OH group.

The BAG, MBAG, MBAGT and MBAGTM exhibited the characteristic absorption bands with no appearance of new peaks. The BAG and MBAG films showed multiple bands that previously explained in topic 4.1.2 and the MBAGT film showed multiple bands that previously explained in topic 4.2.2. The changes in absorption spectrum of the MBAGTM films containing 1, 5 and 10% v/v mangosteen ethanolic extract were as follows. The C-O-C stretching peak were shifted to 1059, 1060 and 1060 cm^{-1} and the O-H and the N-H stretching bands were shifted to 3400,

3352 and 3352 cm^{-1}, respectively. The H-O-H bending peaks were shifted to 1646, 1648 and 1657 cm^{-1} which it also can be assigned to the C=O stretching and the -COO stretching peaks were shifted to 1437, 1442 and 1443 cm^{-1}, respectively. The symmetric of N-H bending peaks were shifted to 1535, 1536 and 1535 cm^{-1} and the C-N stretching peaks were shifted to 1236, 1237 and 1237 cm^{-1}, respectively. The arising of stretching vibrations of C-H group stretching in aromatic ring of both aromatic and alkene at around 2926-2932 cm^{-1} showed that the MBAGTM films contained mangosteen extract. The amplitude of this peaks increased with increasing of the extract content. The shift of this peak could imply weakly interactions between the functional groups of the film and cyclic alkenes in mangosteen extract.

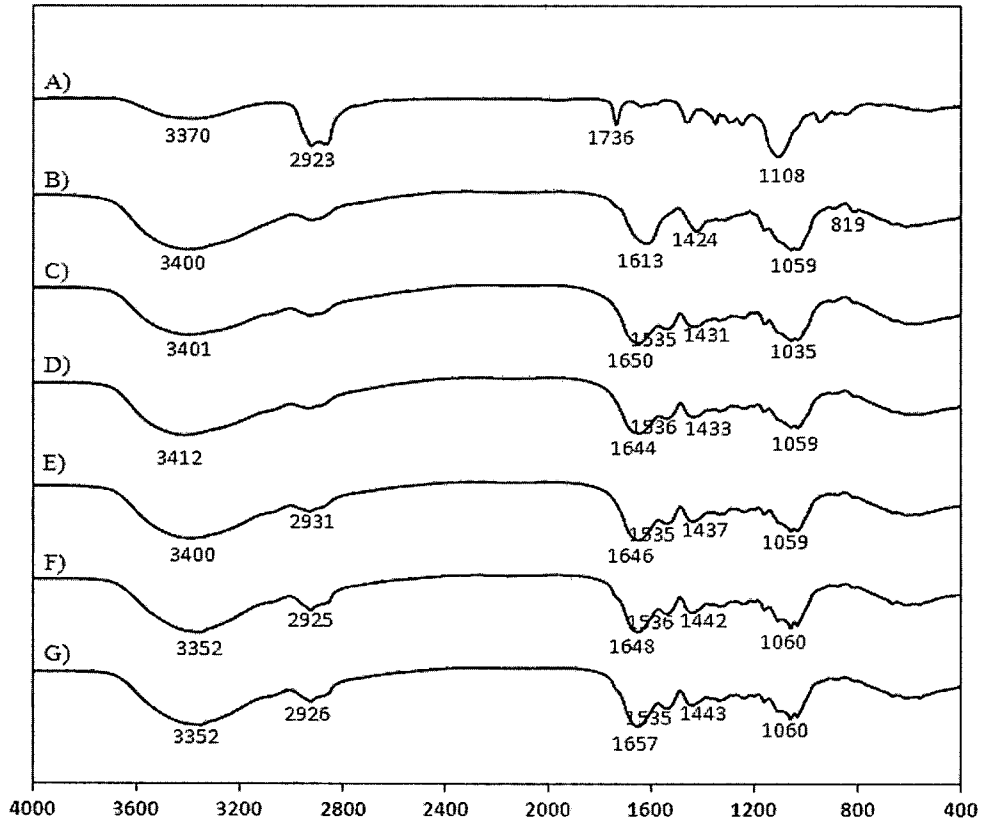

Figure 4.24 FT-IR of mangosteen ethanolic extract (A), the BAG (B), MBAG (C), MBAGT-10 mg (D) and MBAGTM at 1% (E), 5% (F) and 10% (G) v/v concentration of mangosteen ethanolic extract, respectively.

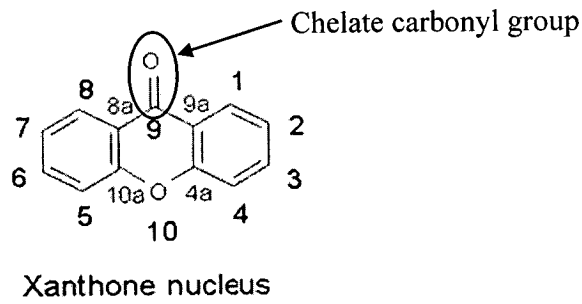

Figure 4.25 Chelating of carbonyl group in the backbone of xanthone (Chaverri et al., 2008)

4.4.3 Water absorption capacity (WAC)

The WAC of the MBAGTM films in DI water is shown in Figure 4.26. The WAC values decreased with the increase of mangosteen ethanolic extract content. The WACs of the BAG, MBAG and MBAGT films were 333.6, 462.2 and 389.9%, respectively, whereas the WACs of the MBAGTM films containing the mangosteen extract at 1, 5 and 10% v/v were 321.9, 282.2 and 269.6% respectively. The ethanolic extract contained hydrophobic compounds which were less hydrophilic than BC, alginate and gelatin and the extract compounds could filled in the micropores of the films, reducing the void volume. Therefore the supplement of mangosteen ethanolic extract reduced the WAC of the films.

It was previously reported that the hydrophobic nature of cellulose could be generated with the presence of hydrophobic substances in cellulose domains (Yamane et al., 2006). For the same reason, with the supplement of hydrophobic compounds from the mangosteen ethanolic extract, the hydrophobic nature of the modified films was enhanced.

However, the WACS of the MBAGTM films were only slightly decreased with the increase of the mangosteen extract from 5% to 10% v/v. Therefore, the addition of the extract more than 5 % might not further lower void volume of the film. On the other hand, the high supplement of the mangosteen ethanolic extract might also have interfering effects on the chemical bonds of the films, resulting in a looser

film structure, which could be a reason for almost equal WAC of the MBAGTM film with the increase of the mangosteen extract from 5 to 10 % (v/v).

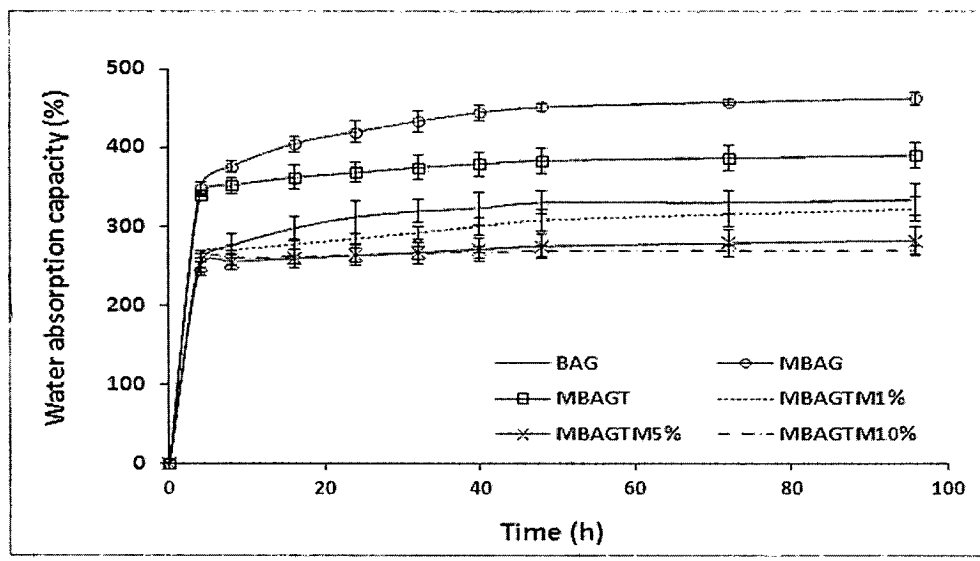

Figure 4.26 Water absorption capacity (%) of the composite films: BAG (——); MBAG (—○—); MBAGT (—□—); MBAGTM1% (·····); MBAGTM5% ( ) and MBAGTM10% (- - -), respectively.

4.4.4 Mechanical properties

Tensile strength (TS) and elongation at break (EB) of the films in dry state of BAG, MBAG, MBAGT and MBAGTM containing the mangosteen extract at 1, 5 and 10% v/v were shown in Figure 4.27 A and B.

Compared to the MBAGT film, the MBAGTM films with 1% v/v of the extract exhibited slightly increased TS and EB to 188.9 MPa and 3.0%, respectively, which could be owing to the effect of filling pores or coating fibrils of the extract compounds on interconnections of network BAG fibrils. Nevertheless, the MBAGTM films with 5 and 10% v/v of the extract exhibited the significant decrease in TS and the increase in EB, which could again be a result of the loosen structure at the high supplement of the mangosteen ethanolic extract as discussed previously in Topic

4.4.3.

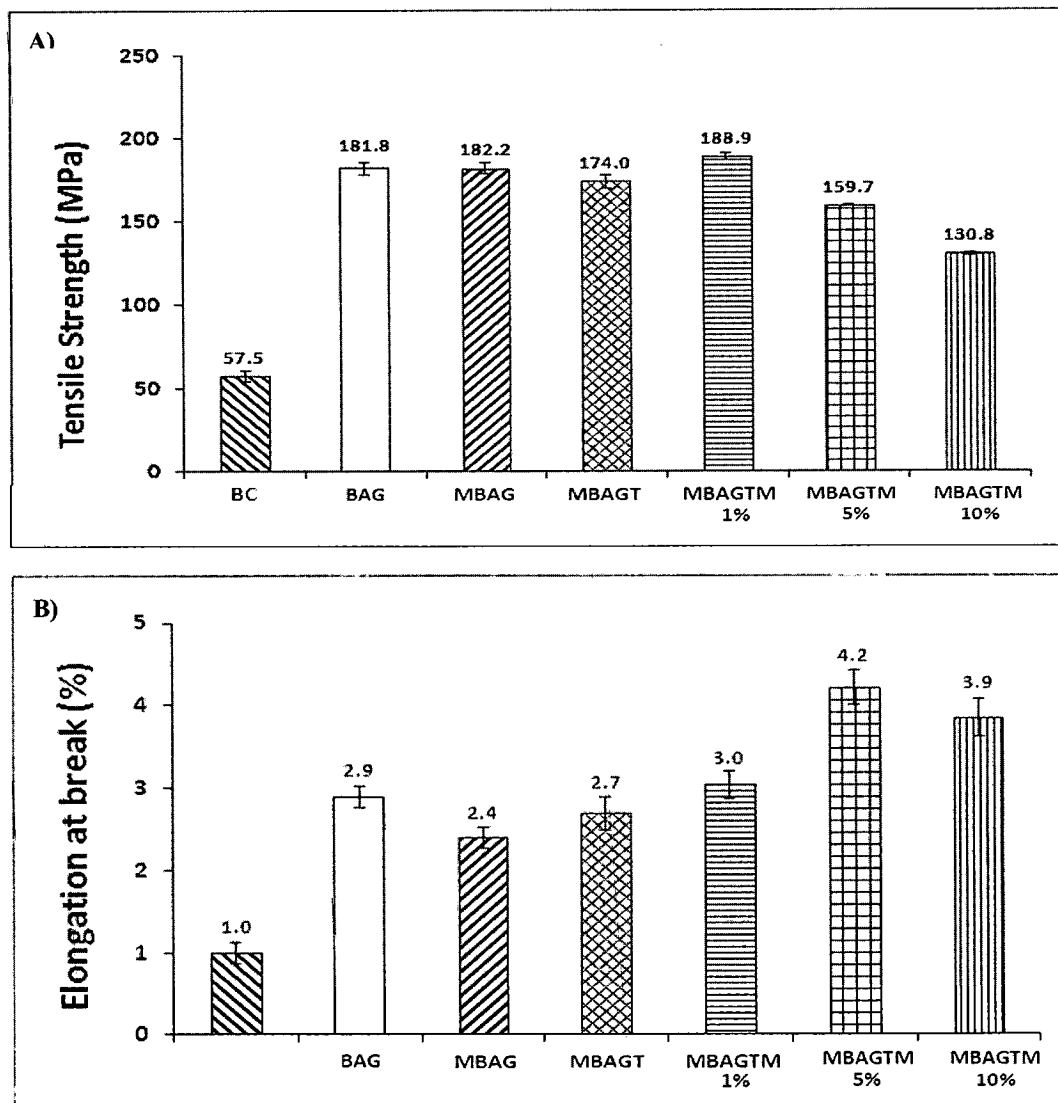

Figure 4.27 Mechanical properties of MBAGTM films in dry state at 1%, 5% and 10% v/v concentration of mangosteen ethanolic extract: Tensile strength (A) and Elongation at break (B).

Tensile strength (TS) and elongation at break (EB) of the films in wet state were shown in Figure 4.28 A and B. In wet state, the TS of the MBAGTM films which contained the mangosteen extract at 1, 5 and 10% v/v was slightly lower than

those of the MBAGT films. The EB of the MBAGTM film at 1% v/v of the mangosteen extract increased to 63.0% but the EB of the films decreased to 46.7 and 47.2% with the further adding the mangosteen extract to 5 and 10% v/v. The TS of the re-swollen was only about 0.11-0.15 of the dry films, whereas the EB of the re-swollen films was about 10-20 folds greater than the dry films. Overall, these results should be a consequence of a very relaxed network structure of the films in wet state.

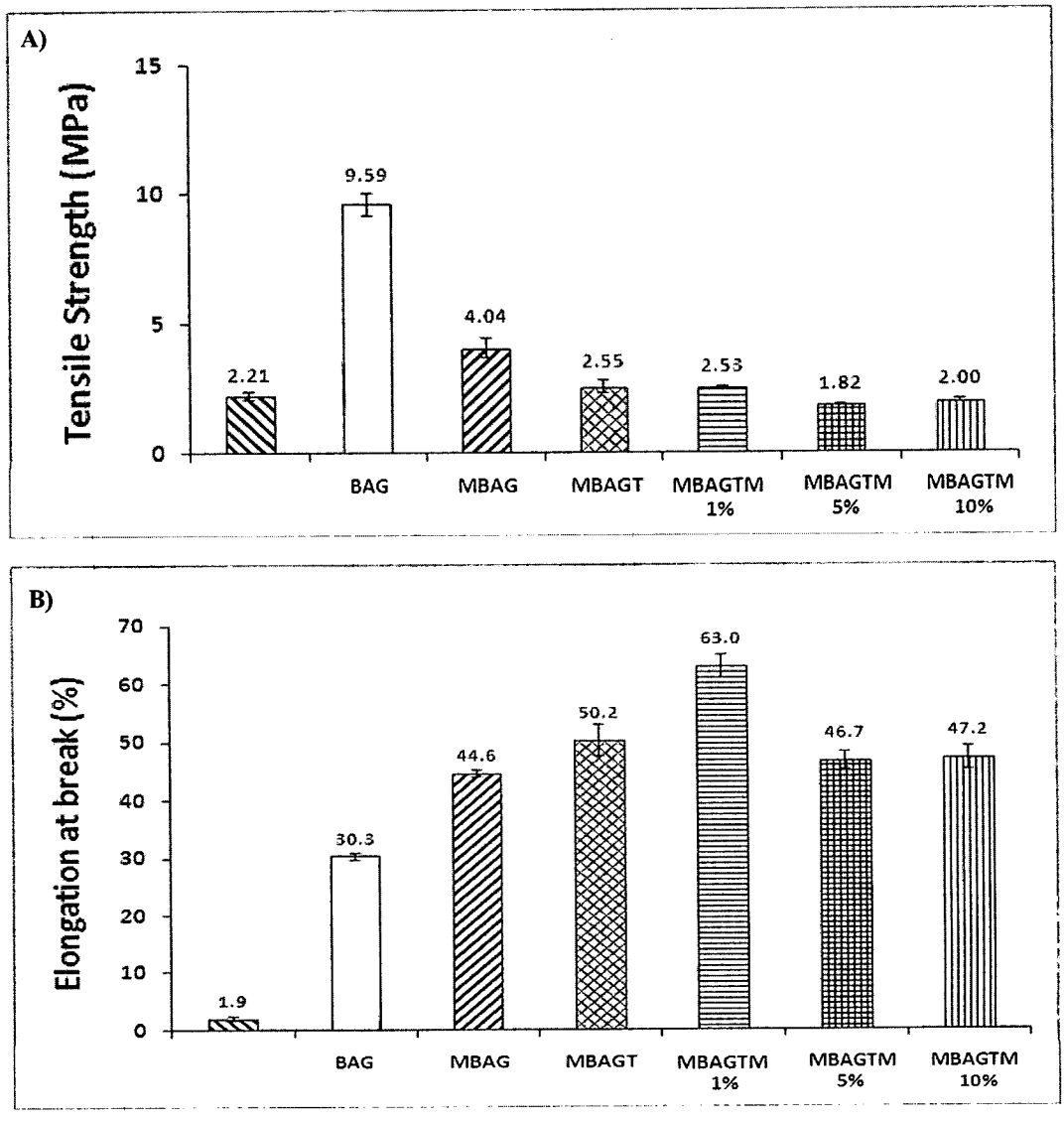

Figure 4.28 Mechanical properties of MBAGTM films in wet state at 1%, 5% and 10% v/v concentration of mangosteen ethanolic extract: Tensile strength (A) and Elongation at break (B).

4.4.5 Scanning electron microscope (SEM)

The SEM photographs of surface morphology of films in dry state at 200 magnifications were showed in Figure 4.29 A, B and C. The surface roughness of nanocellulose fibers of MBAGTM films was still observed but not as much as being observed on the MBAGT films.

SEM photographs in Figure 4.30 (A-F) reveal the surface morphology at 10,000 magnifications of the MBAGTM films in dry and wet states. After adding mangosteen ethanolic extract (1, 5 and 10% v/v) into the mixture slurry, the extract could penetrate into empty space in microporus structures of BC fibrils, alginate and tannic acid cross-liked gelatin. The extract incorporated in the composite films resulting in a smoother surface. Especially the films in dry state, nanocellulose fibrils could barely be observed on the film surface and the thickness of the films increased with noticeable excess extract compounds on the film surfaces.

Compared to the dry films, the re-swollen films exhibited a loose fibril network. The addition of mangosteen ethanolic extract might affect cellulose nanofibril orientation and enhance the free volume for motion of cellulose fibril. Moreover, the MBAGTM, especially a 10% v/v mangosteen ethanolic extract supplement showed small cracks or hairline fractures distributed along some part of BAG fibrils as shown in Figure 4.30 (B, D and F).

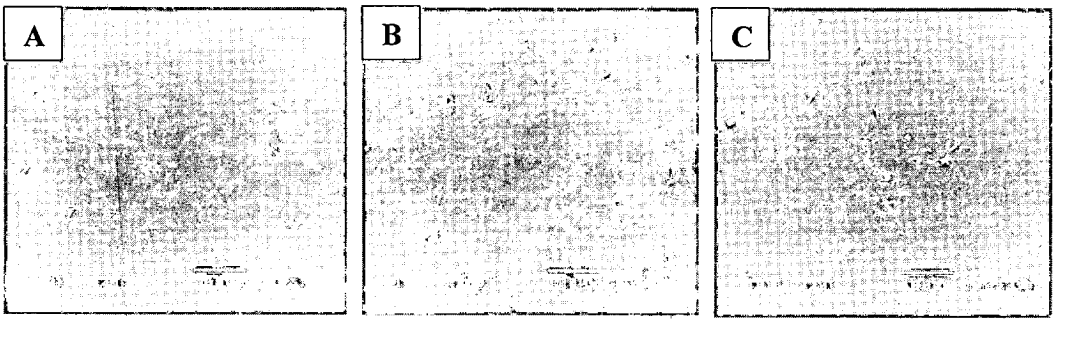

Figure 4.29 SEM images of overview surface morphology at magnification 10 kV 200X of MBAGTM at concentration of 1%, 5% and 10% v/v mangosteen ethanolic extract in dry state.

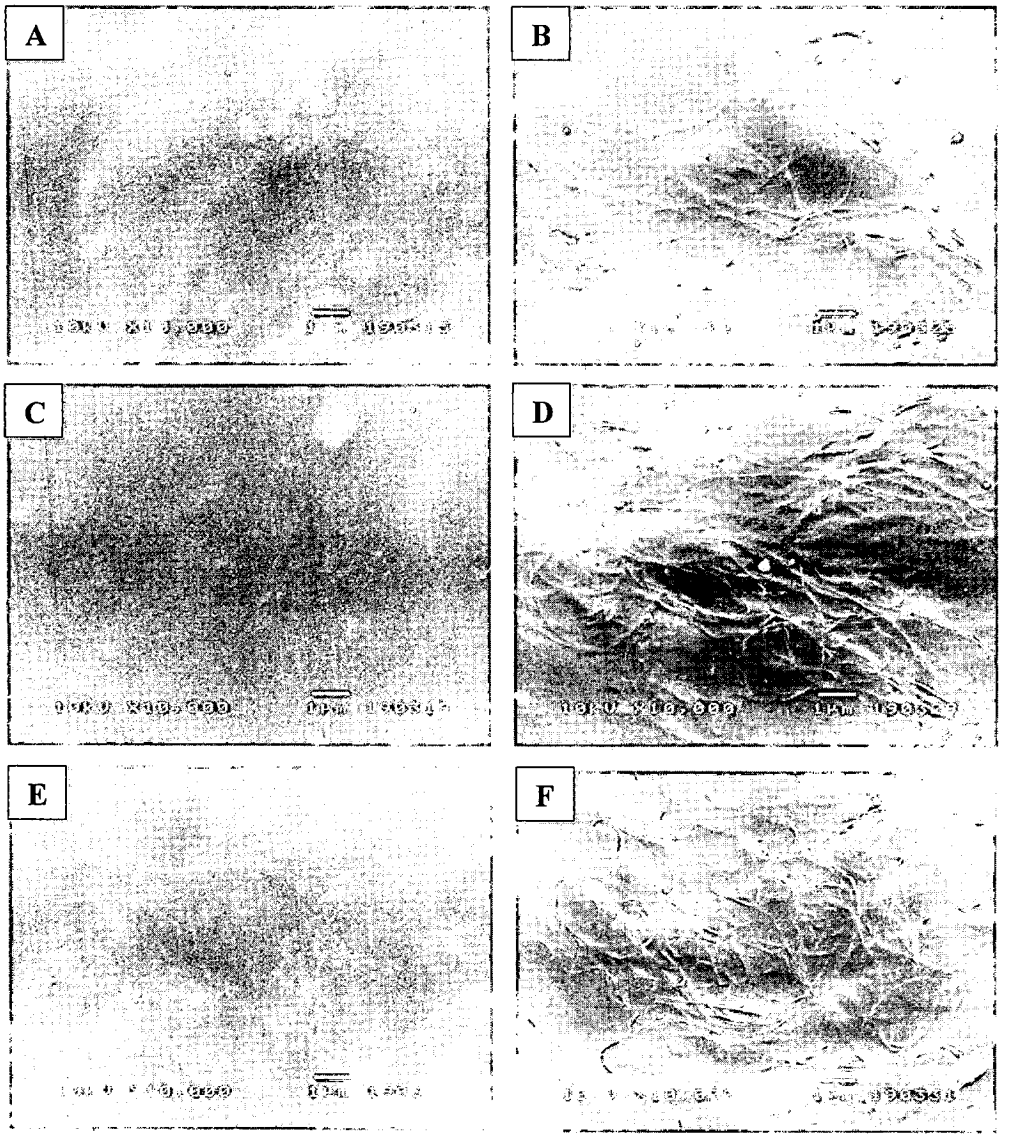

Figure 4.30 SEM images of surface morphology of MBAGTM films in dry (left) and re-swollen (right) forms at concentration of 1% (A and B), 5% (C and D) and 10% (E and F) v/v mangosteen ethanolic extract.

Figure 4.31 illustrates the cross sectional morphologies of the MBAGTM films. As compared to the MBAGT films, each layer thickness of the film sheet of MBAGTM was enhanced, along with the increases of void fraction or free volume and disorder of orientation. Since the compounds in the extract could penetrate into the film sheet and coated on the surface of the sheet, the addition of the mangosteen

extract might increase heterogeneous and hydrophobic characters in the films. The ethanolic extract contained hydrophobic compounds, whereas main components of the BAG film were hydrophilic compounds. Therefore the supplement of the ethanolic extract promoted the heterogeneous compatibility or solubility in the films. It might lead to noticeable increase in free volume space of the modified films (MBAGT films) as shown in the SEM images of film cross-sections (Figure 4.31). Therefore, the addition of the extract enhanced the thickness as well as the inter-space of the sheet layers of the MBAGTM films.

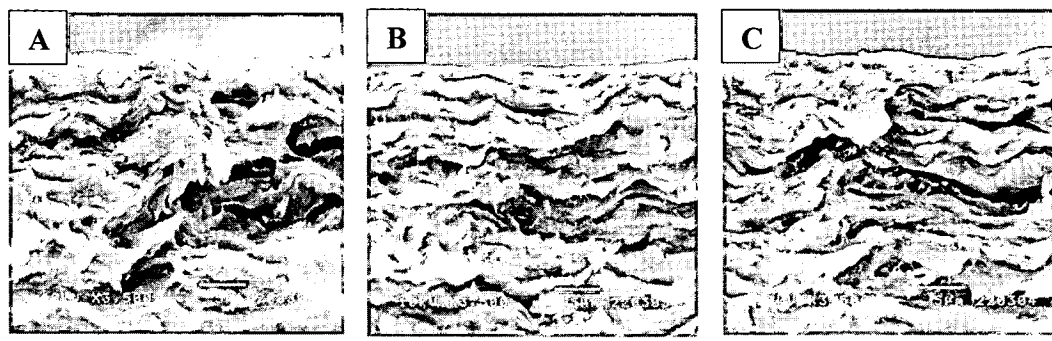

Figure 4.31 SEM images of cross sectional morphology: the MBAGT films in dry state at concentration of 1%, 5% and 10% v/v mangosteen ethanolic extract

4.4.6 X-ray diffraction

The X-ray diffraction (XRD) was used to determine the crystallinity of the films. The XRD patterns and crystallinity (%) of BC, BAG, MBAG, MBAGT and MBAGTM films containing mangosteen ethanolic extract at 1, 5 and 10% v/v were shown in Figure 4.32. The pattern of BC exhibits three main peaks at 2θ of 14.54°, 16.87° and 22.68° (related to more crystalline order), which are corresponding the (1 $\bar{1}$ 1), (1 1 0) and (2 0 0) reflexion planes of cellulose I, respectively, as already reported by Cai and Kim (2010), Retegi et al. (2010) and Phisalaphong et al. (2008). Both gelatin and alginate are amorphous compounds; therefore their crystallinities are extremely low.

The reflexion planes: reflective-angle and d-spacing values of BC, BAG, MBAG, MBAGT and the MBAGTM films are shown in Table 4.2. Except for the three main peaks of BC, all of modified film by sodium alginate, gelatin, tannic acid and mangosteen ethanolic extract showed no other characteristics peaks implying amorphous nature of the other polymers.

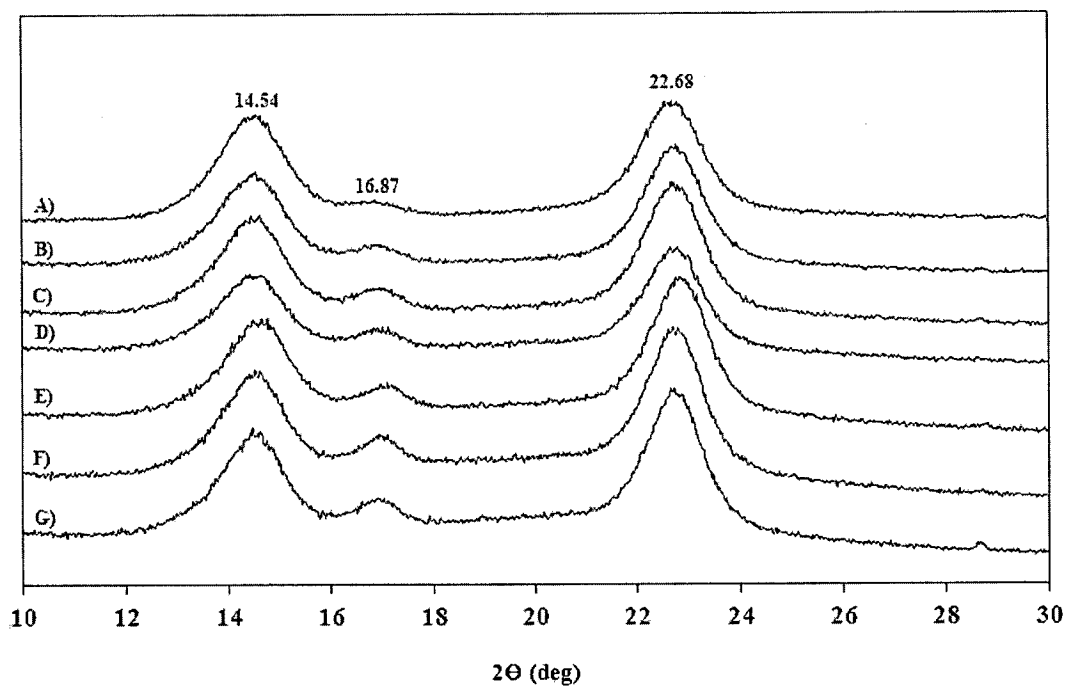

Figure 4.32 The X-ray diffraction (XRD) patterns of BC (A), BAG (B), MBAG (C), MBAGT (D) and MBAGTM films at 1% (E), 5% (F) and 10% (G) v/v concentration of mangosteen ethanolic extract

According to Table 4.3, the degree of crystallinity (%) of BC, BAG, MBAG, MBAGT and MBAGTM at 1, 5 and 10% v/v of the extract was 68.82, 67.68, 71.24, 66.21, 65.93, 59.43 and 59.21 %, respectively. The addition of glycerol as a plasticizer into BAG film (referred as MBAG film) supported the molecular movements and could promote crystallization; therefore, an elevated degree of crystallinity to 71.24 % of the composite MBAG film was obtained. However, the results exhibited that the crystallinity of the films tended to decrease with adding

tannic acid and mangosteen ethanolic extract into the MBAG film. It can be explained by the strong interaction between BC, sodium alginate and gelatin which has destroyed the close packing of the BC molecules for the formation of regular crystallites. Similar observations were previously reported in alginate/gelatin blend films for drug controlled release (Dong et al., 2006). Furthermore, the addition of tannic acid decreased crystallinity of the film due to the enlarged intermolecular interactions between hydroxyl groups in tannic acid and NH_2 side-chain groups in gelatin, which might limit the molecular movements, thus preventing crystallization (Peña et al., 2010).

Table 4.2 The reflexion planes: reflective-angle and d-spacing values of BC, BAG, MBAG, MBAGT and the MBAGTM films

Film sample	**2θ [d(1 $\bar{1}$ 1)]**	**2θ [d(1 1 0)]**	**2θ [d(2 0 0)]**
BC	14.54° (6.09)	16.87° (5.25)	22.68° (3.92)
BAG	14.54° (6.09)	16.89° (5.24)	22.77° (3.90)
MBAG	14.61° (6.06)	16.96° (5.23)	22.68° (3.92)
MBAGT	14.36° (6.09)	17.12° (5.18))	22.66° (3.90)
MBAGTM1%	14.65° (6.04)	17.10° (5.18)	22.84° (3.89)
MBAGTM5%	14.52° (6.10)	16.94° (5.23)	22.70° (3.91)
MBAGTM10%	14.47° (6.12)	17.03° (5.21)	22.73° (3.91)

Table 4.3 Degree of crystallinity (%) of BC (A), MBAG (B), MBAGT (C) and MBAGTM films at concentration of 1% (D), 5% (E) and 10% (F) v/v mangosteen ethanolic extract

Film	**BC**	**BAG**	**MBAG**	**MBAGT**	**MBAGTM 1%**	**MBAGTM 5%**	**MBAGTM 10%**
Crystalline area	9646	9657	10489	8312	11356	12002	11597
Amorphous area	4359	4611	4235	4243	5868	8192	7988
Crystallinity (%)	68.82	67.68	71.24	66.21	65.93	59.43	59.21

4.4.7 Oxygen permeability

Table 4.4 showed the results of the oxygen transmission rate (OTR) of the BAG, MBAG, MBAGT and MBAGTM films (mean values from the duplicate testing) comparing with the commercial film packaging. Due to the extremely small pore diameter of the films in dry state, the corresponding values of OTR were considerably low. The OTR of BAG, MBAG, MBAGT and MBAGTM10% was 0.887, 1.080, 0.764 and 1.100 cc/m^2/day, respectively.

The OTR of films in dry state decreased from the general BC film because of the reduction of pore diameter into nanometer-sized pores, whereas the approximate diameter of oxygen molecule is around 0.36 nm (Kanjanamosit et al., 2009) or 11 Å (Hambleton et al., 2009), so that oxygen could slightly flow through the films.

Generally, the film of sodium alginate is impervious to oils and fats but it is poor moisture barriers and has high oxygen permeability coefficient. On the other hand, hydrogen bonds in gelatin films can be used as the barrier to oxygen. Thus, gelatin adding offers a lower chance of protein oxidation. Gelatin films do not allow oxygen-protein interactions (Krochta and Johnson; 1997) and can significantly prevent lipid oxidation. As shown in the previous SEM images, sodium alginate and gelatin could fill empty space between BC fibrils leading to the decreased pore diameter and consequently, causing the reduction in oxygen permeability of the films. In addition, according to the interpenetrating effects, polymer chains are confined to a smaller volume through strong interactions (electrostatic attractions and intermolecular hydrogen bonding); this could also lead to the reduction of free volume for the interfacial polymers, which takes longer for oxygen molecules to travel through and causes them to have more interactions (Svagan et al., 2012; Gu et al., 2013). Moreover, it was previously suggested that due to the hydrophilic nature of proteins of gelatin, it can limit the resistance to water vapor transmission, but provide excellent oxygen barriers at low relative humidity (Wang et al., 2010).

The addition of plasticizers as glycerol increased the oxygen permeability since glycerol can induce a structural change of the BAG film. Similar observations were previously reported that the addition of plasticizers such as glycerol increased oxygen permeability for polysaccharide films (Sothornvit and Pitak, 2007) such as

HPMC composite films (Imran et al., 2010) and gelatin films (Herring et al., 2010). However, the OTR increased only slightly by adding glycerol to form the MBAG films.

The addition of tannic acid reduced the oxygen permeability because tannic acid could crosslink gelatin, resulted in decreasing free volume space as well as pore diameter of the MBAGT film in dry state. Further addition of the mangosteen ethanolic extract into the films slightly improved the OTR of the films because of the increased free volume as previously discussed in topic 4.4.5.

When compared with the commercial packaging films such LDPE, HDPE, polypropylene, polyester, PET, polyvinyl chloride (plasticized) and polystyrene (PS) as shown in Table 4.4, the OTR of all developed films in this study were within the range of those of commercial packaging films. This result indicated that the BAG and modified BAG films have good potential to be used as packaging films to prevent food oxidation.

Table 4.4 The oxygen transmission rate of the BAG film at a ratio of 60/20/20, the MBAG film, the MBAGT and MBAGTM film (Mean value from duplicate testing) and commercial film packaging (*Modern plastics encyclopedia, 1979-1980)

Material	OTR±S.D. (cc/m^2.day)
BAG	0.887±0.026
MBAG	1.080±0.042
MBAGT	0.764±0.042
MBAGTM10%	1.100±0.000
Low density polyethylene (LDPE)*	500
High density polyethylene (HDPE)*	185
Polypropylene*	150-240
Polyester, PET*	3.0-4.0
Polyvinyl chloride (plasticized)*	2-400
Polystyrene (PS)*	250-350

4.4.8 Water vapor permeability

In the food industry, the difficulty with composite films is the relatively high water vapor permeability. Permeability in packaging is controlled by the diffusivity and solubility of water within the film matrix. Thus implementing food nanotechnology, new organization of firmly linked three dimensional networks can be fabricated to prevent diffusion of water in foodstuffs (De Moura et al., 2009; Imran et al., 2012).

In general, WVTR values for composite films produced from protein and polysaccharide mixtures were lower in comparison to the WVTR values of those films formed from protein alone (Wang et al., 2010). All films were analyzed for water vapor transmission property by following the ASTM E-96. Table 5.10 showed the results of the water vapor transmission rate (WVTR) of the BAG, MBAG, MBAGT and MBAGTM films (using mean values from duplicate testing) comparing with the commercial film packaging. The water vapor transmission rate (WVTR) of BAG, MBAG, MBAGT and MBAGTM10% was 769.00, 793.00, 976.32 and 1402.08 $g/m^2/day$, respectively.

BC is high hydrophilic with a uniform porous structure. Therefore, water vapor could be easier to diffuse though the film resulted in high WVTR.

The WVTR of the BAG film should reduce from BC film because sodium alginate and gelatin wrapped between BC fibril which the ionic crosslinking in sodium alginate reduced polymer segmental mobility as resulting in hard diffusing though the film. It has been previously explained that calcium ions are located in cavities linking two L-guluronic acid chains of alginate; the ability of L-guluronic acid to form an insoluble net makes alginate films a good barrier to water vapor (Olivas and Barbosa-Cànovas, 2008; Hableton et al., 2009). The chemical interaction between water and film materials that resulted in a volume expansion and the ultimately increase of free volume was found to have marked effects on water vapor permeation (Kääriäinen et al., 2011).

With the addition of glycerol as plasticize, the WVTR of the MBAG film was slightly higher than the unplasticized film. The incorporation of glycerol provoked a reorganization of the BAG network, which became less dense with a larger free

volume, facilitating greater mobility and as a consequence, greater WVTR was obtained. The approximate diameter of water molecule is 2.4 Å (Hambleton et al., 2009). Glycerol plasticized film had given significantly higher permeability, which may be caused by the higher number of available polar (-OH) groups in MBAG composite films. In general, the addition of a plasticizer modifies the properties of the film by reducing the intermolecular bonds between the polymer chains, thus increasing the WVTP of the films. The water also plays the role of plasticizer in hydrophilic coatings and the density or local viscosity decrease promoting the diffusing molecules mobility (Guilbert and Biquet, 1996).

For the MBAGT film, the addition of tannic acid to crosslinked gelatin showed a slightly positive impact on the WVTR. It could probably be assumed that polar groups that were many hydroxy groups of tannic acid compounds incorporated with water, so that the apparent WVTR did not change or slightly changed with adding tannic acid. Similar observations were previously reported that tannic acid slightly increased WVTP of gelatin films (Cao et al., 2007) and addition of tannic acid, caffeic acid and ferulic acid at all levels increased WVTP of resulting films (Nuthong et al., 2009). Furthermore, with adding mangosteen ethanolic extract into the films, the WVTR increased. Because the extract is hydrophobic compound and the main components of the film are hydrophilic compounds, therefore the heterogeneous compatibility or solubility occurred, which could lead to increased free volume space of MBAGTM film as previously discussed in Topic 4.4.5. Moreover, the excess mangosteen ethanolic extract caused small crack or fracture on surface films, which might have small effect on WVTR and OTR of the films. Mangosteen ethanolic extract is recognized to improve the water barrier properties of biopolymer films due to its hydrophobic nature and reduce the water sorption capacity of the films. However, it was found that the increase of free volume had marked effects on WVTR of the MBAGTM films; as a result the WVTR of the modified film significantly enhanced.

Table 4.5 The water vapor permeability measurement of the BAG film at a ratio of 60/20/20, modified the films and BAGM film (Mean value from duplicate testing) and commercial film packaging (*Modern plastics encyclopedia, 1979-1980)

Material	WVTR±S.D. ($g/m^2.day$)
BAG	769.00±1.41
MBAG	793.00±1.41
MBAGT	976.32±13.58
MBAGTM10%	1402.08±20.36
Low density polyethylene (LDPE)*	1.0-1.5
High density polyethylene (HDPE)*	0.3
Polypropylene*	0.7
Polyester, PET*	1.0-1.3
Polyvinyl chloride (plasticized)*	5-30
Polystyrene (PS)*	7-10

4.5 Antimicrobial activities

4.5.1 The minimum inhibitory concentration test (MIC) and the minimum bactericidal concentration test (MBC)

The minimum inhibitory concentrations (MIC) and minimum bactericidal concentrations (MBC) of mangosteen ethanolic extracted from *G. mangostana* fruit pericarp (in ethanol solution with tween-80) and tannic acid was shown in Table 4.6.

The antimicrobial activity of mangosteen ethanolic extract at concentrations of 5.84, 2.96, 1.46, 0.73, 0.365, 0.1825, 0.09125, 0.0456, 0.0228 and 0.0114 mg/ml was determined on four selected strains of pathogenic bacteria using a broth microdilution method. To compare the antimicrobial potential of different samples, the results of the lowest concentration of extract required to completely inhibit the growth of the microorganisms at concentrations of 1×10^8 CFU/mL (MIC).

The results of MIC exhibited that mangosteen ethanolic extracted and tannic acid could inhibit bacteria in food; *Escherichia coli*, *Salmonella typhimurium*, *Listeria monocytogenes* and *Staphylococcus aureus*. The MIC for mangosteen ethanolic extract possessed at 1.46 mg/ml concentration for *Escherichia coli* and *S. aureus*, and at 0.73 mg/ml concentration for *S. typhimurium* and *L. monocytogenes*. Tannic acid possessed at 30 mg/ml concentration for *E. coli*, *S. typhimurium* and *S. aureus*, and at 15 mg/ml concentration for *L. monocytogenes*.

The MBC for mangosteen ethanolic extract possessed at 1.46 mg/ml concentration for all bacteria, whereas tannic acid possessed at 30 mg/ml concentration for *E. coli*, *S. typhimurium* and *S. aureus*, and at 15 mg/ml concentration for *L. monocytogenes*. Antimicrobial agents with low activity against an organism had a high MIC while a highly active antimicrobial agent gave a low MIC. These results indicated that the mangosteen ethanolic extract exhibited more effective antibacterial activity against the bacteria than tannic acid.

Table 4.6 The minimum inhibitory and minimum bactericidal concentrations (MIC and MBC) of mangosteen ethanolic extract and tannic acid

Microorganisms	Mangosteen ethanolic extract		Tannic acid	
	MIC (mg/ml)	MBC (mg/ml)	MIC (mg/ml)	MBC (mg/ml)
E. coli (−)	1.46	1.46	30	30
S. typhimurium (−)	0.73	1.46	30	30
L. monocytogenes (+)	0.73	1.46	15	15
S. aureus (+)	1.46	1.46	30	30

4.5.2 Antimicrobial assay

The study on antimicrobial activities of MBAGTM films containing mangosteen ethanolic extract against bacteria consisted of *E. coli*, *S. typhimurium* and *S. aureus* and fungi as *A. niger* was evaluated by Disc diffusion method (Voravuthikunchai et al,. 2004). The films containing mangosteen ethanolic extract did not show clear inhibition zones surrounding the film discs in the agar for all microbial tests as shown in Table 4.7, 4.8 and Figure 4.33, 4.34.

Although the disc diffusion method is a common test for antimicrobial activities, the disc diffusion assay has no meaning or provides very poor results for some certain components. According to this method, in order to determine antimicrobial activity, it is required diffusion of antimicrobial agent at certain distance in the agar (or medium). Because diffusion is influenced by molecular weight and other properties such as polarities of the test components and the medium, the result from the evaluation can be very poor for components with non-or low diffusion in the agar. Non polar compound, very high molecular weight compound or compound entrapped in the film does not (or slightly) diffuse in agar, thus it does not produce clear zones. These results indicated that the mangosteen ethanolic extract might not or

only slightly released from the MBAGTM films and barely diffused in the agar. It was probably encapsulated and restrained in the films.

Table 4.7 Antimicrobial activities of MBAGTM films against *E. coli*, *S. typhimurium* and *S. aureus*

Microorganisms	Sample	Clear zone (mm)
E. coli	MBAGTM1%	0
	MBAGTM5%	0
	MBAGTM10%	0
S. typhimurium	MBAGTM1%	0
	MBAGTM5%	0
	MBAGTM10%	0
S. aureus	MBAGTM1%	0
	MBAGTM5%	0
	MBAGTM10%	0

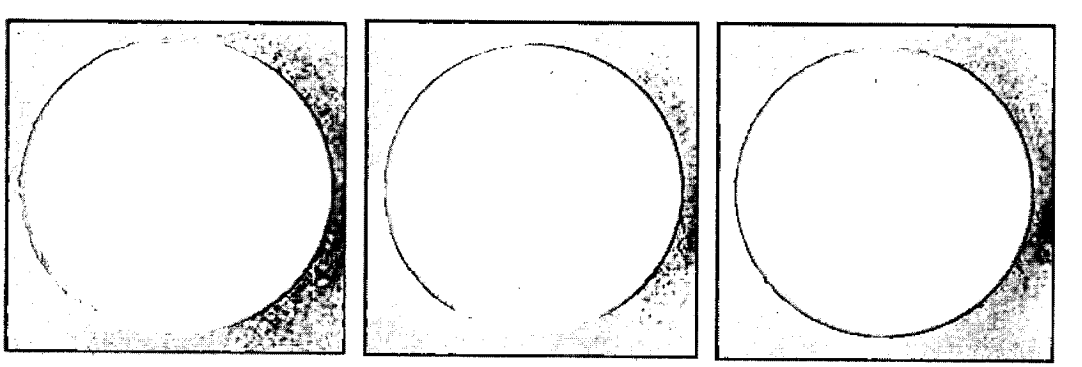

E. coli

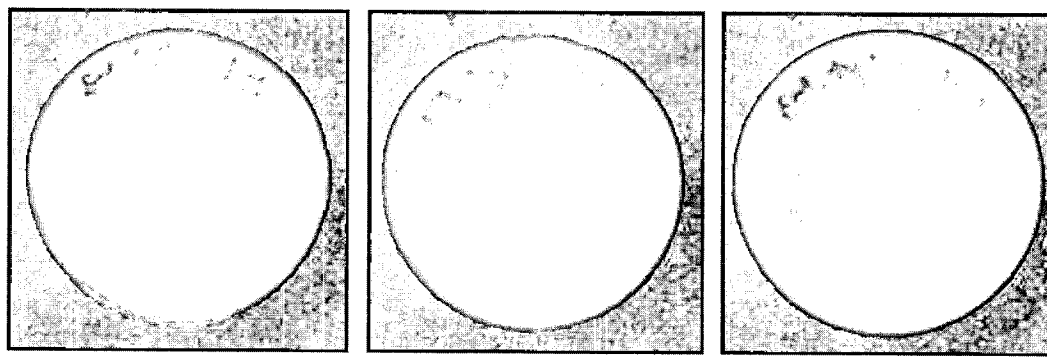

S. typhimurium

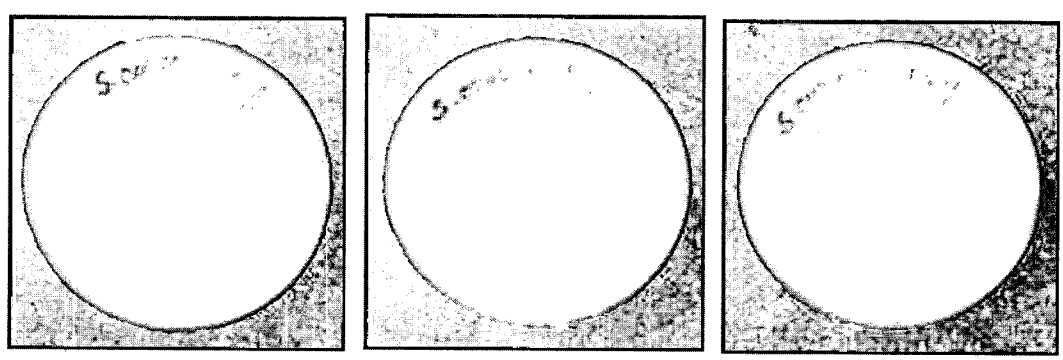

S. Aureus

Figure 4.33 Inhibitory effect of the MBAGTM samples at 1%, 5% and 10% v/v concentration of mangosteen ethanolic extract on the growth of bacteria for 24 h incubated at 37 °C

Table 4.8 Antimicrobial activities of MBAGTM films against *Aspergillus niger*

Microorganisms	Sample	Observed growth
		Grade
A. niger	MBAGTM1%	5
	MBAGTM5%	5
	MBAGTM10%	5

* Grade was used as a measurement of fungal growth: 0 = none, 1 = only apparent under microscope, 2 = trace (<10%), 3 = light growth (10-30%), 4 = medium growth (30-60%) and 5 = heavy growth (> 60%)

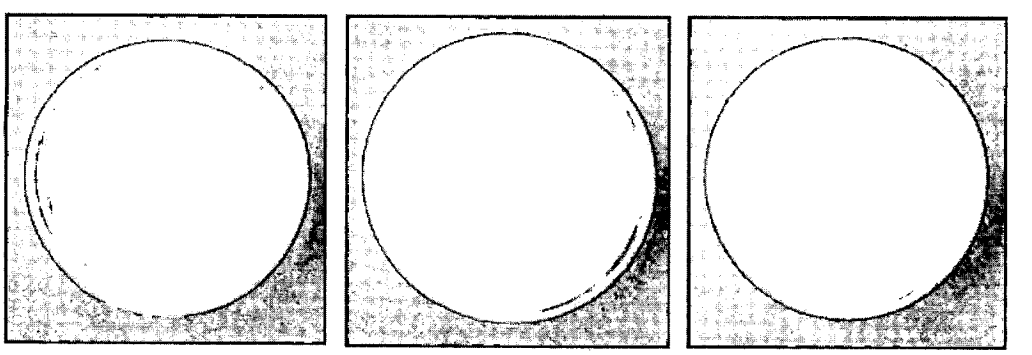

Figure 4.34 The growth of *A. niger* on the MBAGTM specimens, at 30°C at the end of the incubation 7 days

4.6 Absorption and release of bioactive compounds from MBAGTM films

4.6.1 Actual amount of bioactive compounds (phenolic compound and mangostins ethanolic extract)

The summaries of the actual amount of bioactive compounds that were added into MBAGTM films are shown in Table 4.9. The total amount of bioactive compounds in the MBAGTM film were determined to evaluate the holding capacity of the extract in the MBAGTM film and use for analysis of the release characteristics of the mangosteen extract. The MBAGTM at 1, 5 and 10% v/v concentrations of mangosteen ethanolic extract contained phenolic compounds (gallic acid equivalents) at 1.065±0.015, 62.414±0.314 and 102.005±0.635 mg/cm^3 of MBAGTM film and mangostins as 18.149±0.272, 127.256±0.356 and 237.466±0.393 mg/cm^3 of MBAGTM film, respectively. These results exhibited that phenolic compounds and mangostins increased with increasing the extract concentration.

Table 4.9 Actual amount of bioactive compounds in the films

Films	Bioactive compounds	Actual amount in MBAGTM film (mg/cm^3)
MBAGTM1%	Phenolic compounds (GAE)	1.065±0.015
MBAGTM5%		62.414±0.314
MBAGTM10%		102.005±0.635
MBAGTM1%	Mangostins (AME)	18.149±0.272
MBAGTM5%		127.256±0.356
MBAGTM10%		237.466±0.393

4.6.2 Release of bioactive compounds (phenolic compound and mangostins ethanolic extract)

In this study, the cumulative release profiles of bioactive compounds from MBAGTM films containing mangosteen ethanolic extracts were reported as the percentage of the weight of bioactive compounds (phenolic compounds expressed as gallic acid equivalents (GAE) and mangostins expressed as α-mangostin equivalents (AME)) released divided by the actual weight of bioactive compounds containing in MBAGTM films. Acetate buffer at pH 5.6 and Phosphate buffer saline (PBS) at pH 7.4 were used as the solutions.

The cumulative releases of phenolic compounds from MBAGTM films into acetate buffer and PBS are shown in Figure 4.35 A and B. The MBAGTM films modified by supplementation of mangosteen ethanolic extracts with various concentrations of 1, 5 and 10% v/v were investigated for the total amount of released phenolic compounds after the end of total immersion (at 72 h). The results showed that the percentage of cumulative release of phenolic compound from the MBAGTM films at 1, 5 and 10% (v/v) of mangosteen ethanolic extracts were 4.98, 0.09, and 0.05% in the acetate buffer solution at pH 5.6 and 4.89, 0.09, and 0.05% in the PBS buffer solution at pH 7.4, respectively. The percentage of cumulative release of mangostins from the MBAGTM films at 1, 5 and 10% v/v (v/v) of mangosteen ethanolic extracts were 0.53, 0.12, and 0.06% in the acetate buffer solution at pH 5.6 and 1.25, 0.27, and 0.07% in the PBS buffer solution at pH 7.4, respectively (Figure 4.36 A and B). Overall, the releases of phenolic compounds and mangosins from MBAGTM films mainly occurred within 6 h of the immersion. No significant difference of the release of phenolic compounds in the buffers pH 5.6 and pH 7.4, whereas mangosteens released more in the buffer pH 7.4. The releases of phenolic compounds and mangosins from the MBAGTM were very low, especially from the films with high content (5-10%v/v) of mangosteen ethanolic extracts. It was suggested that the accumulation of extract compounds at high concentrations might form agglomerated granules within the cross-linked films and prevented the release of the components.

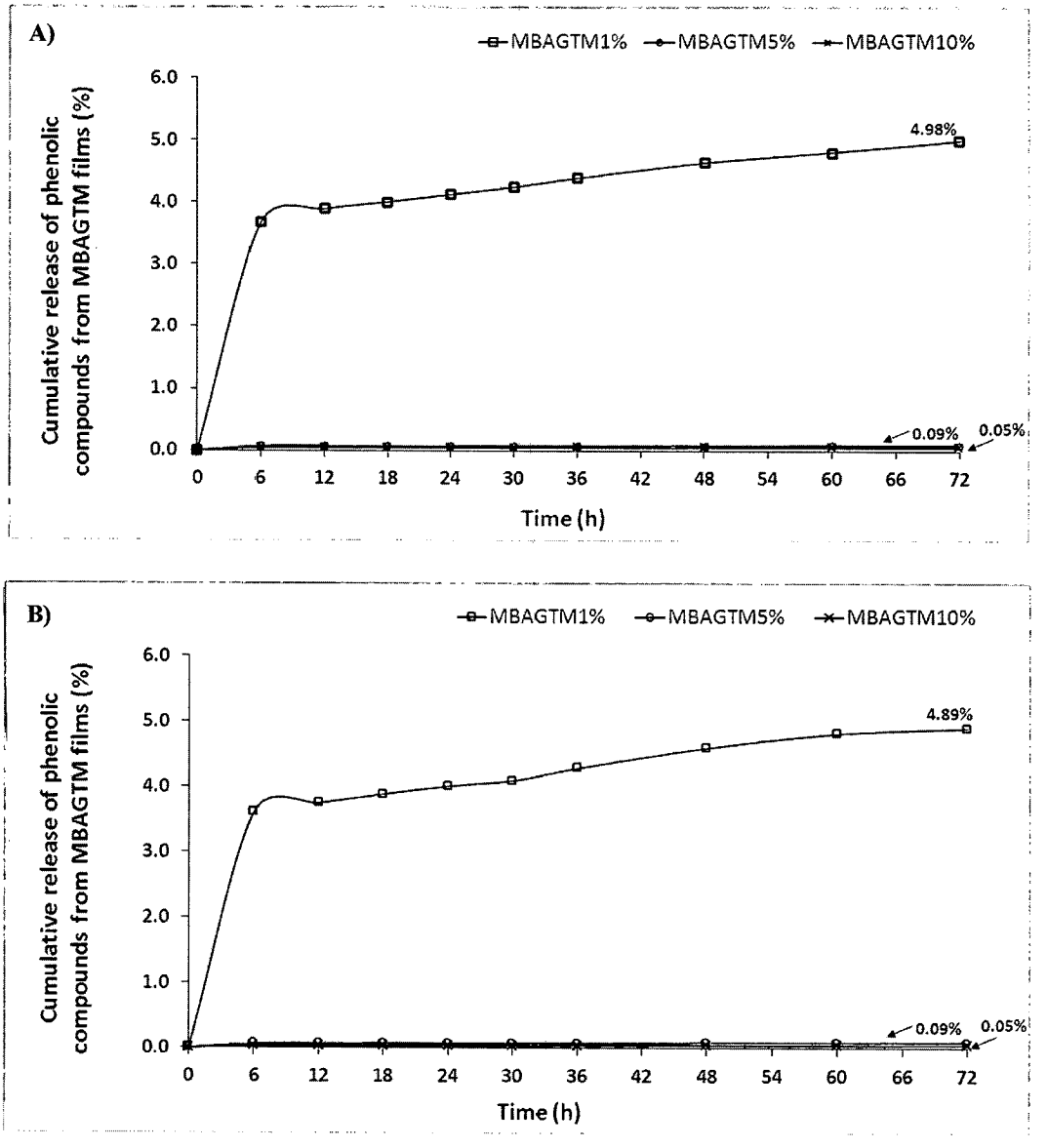

Figure 4.35 Cumulative release profile of phenolic compound from MBAGTM films in acetate buffer at pH 5.6 (A) and PBS at pH 7.4 (B) reported as the percentage of the weight of phenolic compound (GAE) released divided by the actual amount of phenolic compound; MBAGTM at 1% (⊣□⊢), 5% (⊣○⊢) and 10% (⊣×⊢) v/v, respectively

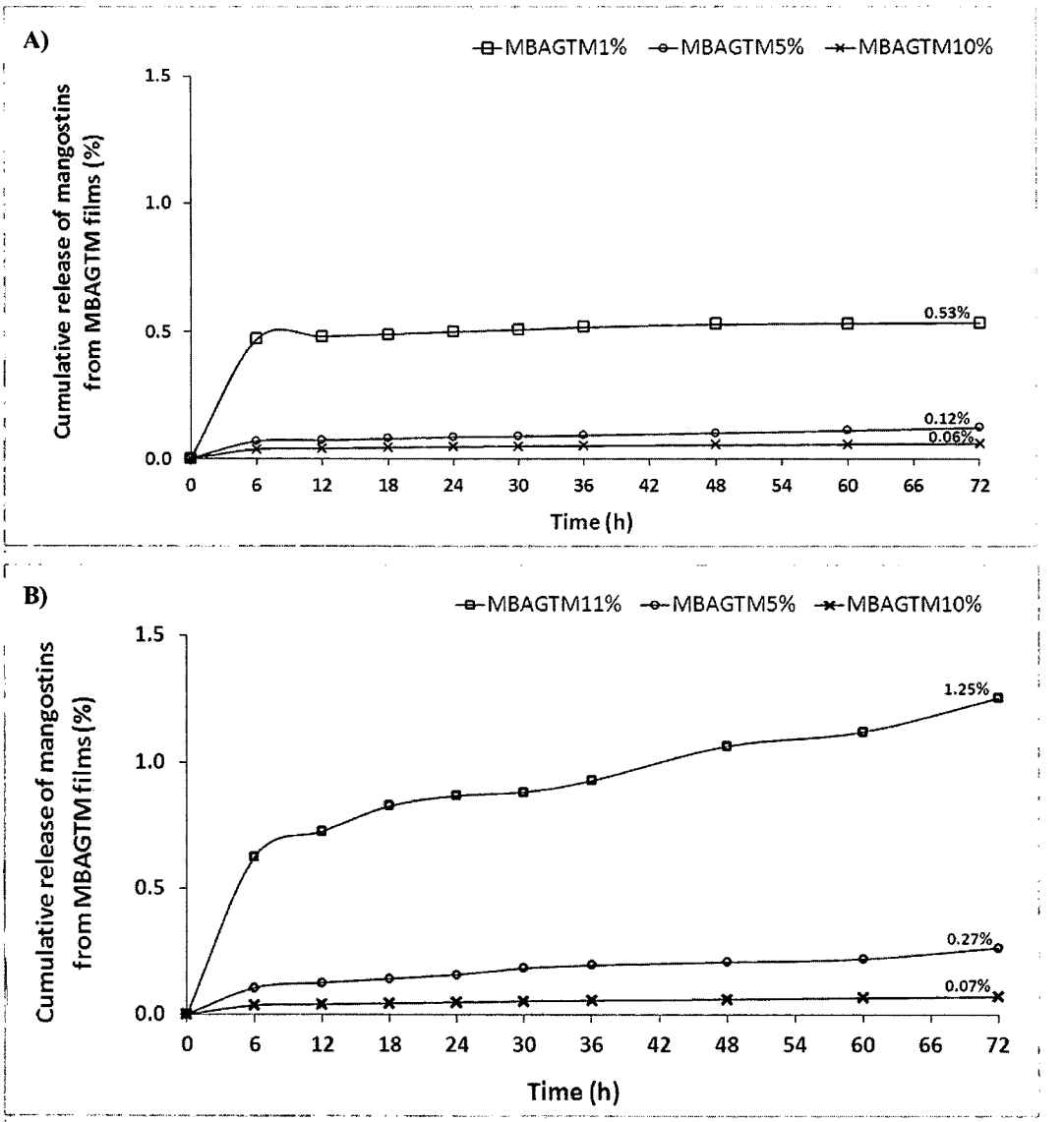

Figure 4.36 Cumulative release profile of mangosins from MBAGTM films in acetate buffer at pH 5.6 (A) and PBS at pH 7.4 (B) reported as the percentage of the weight of mangosins (AME) released divided by the actual amount of mangosins; MBAGTM at 1% (—□—), 5% (—○—) and 10% (—×—) v/v, respectively